HYPERSONIC FLIGHT SIMULATION: AERODYNAMICS

by

J. Leith Potter

von Karman Gas Dynamics Facility

ARO, Inc.

INTRODUCTION

In this lecture an attempt is made to partially assess the current status and direction of laboratory simulation of the aerodynamics of full-scale, hypersonic flight. Problems of simulation related to establishing satisfactory flow fields and the determination of the basic aerodynamic quantities consisting of pressures, forces, and moments, on scale models in these laboratory environments are discussed. In addition, some questions arising in extending scale-model data to full-scale are noted. Other important hypersonic simulation problems are the subjects of later lecturers.

The Role of Aerodynamic Simulation

Inasmuch as the role of simulation in hypersonic aerodynamics has always seemed rather clearly established, it was a temptation to give that aspect of the subject only little attention. After all, the

Wright brothers used a wind tunnel such as the replica shown in Fig. 1. However, opinions recently have been voiced which imply that hypersonics as a research subject is rapidly losing its importance. At the risk of assuming excessive authority, the speaker will venture to place those remarks in which he believes to be the proper context.

More specifically, it does seem true that many of the problems faced by designers of aerospace vehicles once again lie between the subsonic and low-supersonic speed regimes. Examples may be found in the landing of lifting bodies returning from space, drag reduction of supersonic transports, inlet design for air breathing engines, and transonic and supersonic aero-thermo-elastic problems, to name only a few. There is now reasonably adequate understanding, though not necessarily a design solution or precise method of calculation, of most of the well-known hypersonic flow phenomena, e.g., low lift-to-drag ratios and high heating rates. This circumstance exists, in part, because of the degree of Mach number independence and the strong-shock simplifications in hypersonic flow, the essentially perfect-gas behavior which may be assumed in a large range of hypersonic aerodynamic problems, and a formidable effort involving skilled manpower and experimental facilities. Thus, it is not unreasonable to conclude, as others have done, that the unsolved problems in subsonic, transonic, and supersonic flow regimes deserve renewed attention. Furthermore, simulation facilities for these regimes are few in number and sometimes inadequate when tests of unusual new configurations are desired, e.g., V/STOL craft. On the contrary, if one overlooks several

significant points, it may seem that hypersonic wind tunnels providing Mach numbers of 5 to 25 are available in adequate numbers. The significant points alluded to in the last sentence refer to the rather general failure of these current hypersonic tunnels to provide real-gas simulation and the full-scale free-flight range of highest and lowest Reynolds numbers.

Clearly, it may be said that certain by-passed aerodynamic problems related to lower-speed flight indeed deserve renewed attention at the possible expense of effort in hypersonic areas. Also, except for conditions of extreme Reynolds numbers, perfect-gas laboratory simulation facilities seem adequate. Development of facilities substantially simulating real-gas effects of super-orbital speeds and permitting collection of all needed data represents a great difficulty, and much remains to be done. Following from these statements, the need for construction of new hypersonic aerodynamic simulation facilities appears diminished in the category of facilities which provide Mach number but not extreme Reynolds number or real-gas simulation. On the other hand, the role of newer facilities having the capability to simulate less well explored areas of hypersonic aerodynamics cannot beooverlooked when we know that the first craft planned to return to Earth from lunar and interplanetary flights must be very conservatively designed and inefficient owing to lack of precise aerodynamic data. For example the severe requirements pertaining to guidance accuracy for shallow-angle entry and aerodynamic braking in planetary atmospheres may be relieved by further improvements in lift-to-drag ratios

of hypersonic bodies. Also, there now exists roughly a ± 40 percent scatter in heat transfer rates measured at velocities above 20,000 fps. As in the past, it is expected that simulation, more often only partial simulation, in aerodynamic laboratories will provide a large share of the necessary knowledge.

Of course, it is obvious that ground based laboratories alone cannot enable the accomplishment of every investigation. For example, composition and properties of planetary atmospheres are better established by flight of survey vehicles. Also, as long as ground facilities are deficient in speed generated, or in simulation of any other important parameter, certain free-flight experiments are needed. A most interesting example is the use of recorded meteor luminosity and trajectory data to deduce heating rates as described by H. J. Allen in Ref. 1, pp. 1-41.

It may be assumed that the foregoing statements too strongly reflect one individual's personal beliefs. The lecturer is fortunate in being able to refer to a written account of a panel discussion which dealt largely with the role of simulation facilities (Ref. 1, pp. 745-778). Study of that source is recommended. Some of the strong and weak points of laboratory simulation vis-a-vis full-scale free-flight are brought out, and the substantial role of aerodynamic simulation in future developments is clearly indicated in the discussion which is reported in Ref. 1.

No single type of experimental facility stands above all others. Certain types of simulation devices have earned roles that will remain well established although their further development seems of limited

importance. Attention is here confined to facilities not now abundantly represented in the family and which are needed to support hypersonic flight of aerospace vehicle.

FLOW FIELDS

This section is devoted to discussing some of the problems of creating in a laboratory the types of flow fields necessary for adequately simulating the aerodynamics of hypersonic flight. As a prelude to this task, it is obvious that the flow-field conditions expected in full-scale free-flight must be established as accurately as possible. In a fine display of foresight, the organizers of this Conference laid the groundwork for this year's meeting, beginning with the 1961 Conference on Physics of the Solar System and Reentry Dynamics (Ref. 2).

References 1-10*, including the work of many authors, represent a few of the more general or documentary sources of information on characteristics of flow fields and aerodynamic problems relevant to hypersonic flight. Many more references are listed therein. Although not all of the included papers pertain to flow fields under hypersonic conditions, knowledge useful in regard to low-density aerodynamic simulation also may be found in Refs. 11-14, which concern the past

---

*Here, as in other parts of these notes, no pretense of an exhaustive reference list is intended. Where possible, only more recent publications are indicated.

four Symposia on Rarefied Gas Dynamics.

The remainder of this section is devoted to discussion of some selected problems which arise in trying to produce laboratory flow fields for simulating real-gas and either high- or low-Reynolds number phenomena under hypersonic conditions. Actually, many of the comments apply to general aerodynamic laboratory experimentation. Because so much has been written lately concerning simulation of real-gas effects, the problems of simulation related to extremes in Reynolds number, particularly low Reynolds number, will receive most attention. This arrangement recognizes not only the areas of discussion wherein the lecturer is afforded an opportunity to mention his own work, but also the close connection between real-gas phenomena and the topics of later lecturers. References are cited for more extensive and detailed information.

Real-Gas Effects in Aerodynamic Simulation

Although not proposed to be discussed at any length in the present lecture, it is impossible to ignore real-gas effects which are related to other questions to be addressed at this time. Those not familiar with the general subject of real-gas and nonequilibrium processes in gas dynamics simulation will find numerous earlier sources of information, e.g., the papers in the sections entitled "Experimental Techniques" in Ref. 3 (particularly the paper by Hertzberg, et al.) or in Refs. 1, 4, 5, and 11-19. The paper by Lordi and Mates, listed but

not included in Ref. 16, is of much interest. It has been published as Ref. 20. Subsequent lecturers will, no doubt, add to these references.

Real-gas effects often would not be such a problem to aerodynamicists if thermo-chemical nonequilibrium of the gas medium were not encountered. Because the degree of nonequilibrium is a function of the number of collisions allowed among gas particles in a flow field, both density and scale are important. Thus, the possibility of nonequilibrium forces us to consider duplicating free-flight flow fields to an extent not previously necessary. Figure 2 shows the altitude-velocity regime of nonequilibrium chemical-kinetics for conditions representative of a blunt-nose stagnation region in the Earth's atmosphere. The lecturer knows of no complete scaling for nonequilibrium flow. Then, to produce the free-flight flow fields for cases falling within the nonequilibrium regions, the laboratory facility must essentially duplicate not only the flow-field conditions but also the flow-field dimensions! While it may be shown that certain conditions sometimes permit relaxation of this extreme stand in regard to simulation, the general situation is as difficult as the previous statement implies. Figure 3, prepared by C. H. Lewis of ARO, Inc., shows the map of isentropic stagnation pressures and temperatures corresponding to flight in part of the regimes covered in Fig. 2. Comparison of these figures leads to the immediate conclusion that the conditions required for duplicating the higher free-flight speeds become impossible for conventional wind tunnels wherein a high-pressure, high-temperature gas is expanded from a reservoir to hypersonic speeds.

This is demonstrated by Fig. 4, which is representative of current technology insofar as one of the major problems in wind tunnel design is concerned. Even the impulse-type tunnels cannot achieve the levels of total pressure and temperature desired. There is one type of facility that can far exceed others in this respect, namely the aero-ballistic range. However, difficulty of measureing local flow quantities on the model or in its flow field greatly reduces the utility of aero-ballistic ranges. Actually, another type of facility should be included in this category; the counterflow system where a gun fires a model upstream in the expanded flow of a shock tunnel has many of the advantages and handicaps of an aero-ballistic range. Since none of these devices satisfy all requirements and each possesses certain advantages and disadvantages when compared with others, there is need to use all types. It is not necessary to dwell on the economic aspects of construction of large or long-running wind tunnels capable of high pressures, temperatures, and Mach numbers simultaneously.

Even if it is accepted that full matching of flow-field conditions is not now feasible when the more extreme speeds are of concern, much trouble remains in producing wind tunnel conditions that legitimately qualify as "hypervelocity." If we consider that term to denote speeds great enough to create significant real-gas effects, say dissociation in the shock layer of a model, it is likely that dissociation and vibrational excitation must exist in the setting section of the wind tunnel. Under such circumstances, it may often be found the recombination or

even the speedier relaxation of vibration does not keep pace with the decrease in translational and rotational temperatures as the gas expands down a hypersonic nozzle of reasonable length.

When one tests under conditions wherein nonequilibrium may be a factor, calibration of the nozzle flow is more difficult and requires far more work by the aerodynamicist. Some examples of calibration procedures used may be found in Refs. 16, 21 - 23. Low densities and high Mach numbers further complicate the diagnosis of real-gas flows because they make certain measurements difficult.

High reservoir pressures are the best medicine for nonequilibrium troubles in wind tunnel flows, but there are practical limits. Figure 5, available through the courtesy of J. D. Whitfield of ARO, Inc., shows how the required wind tunnel reservoir pressure increases with test section velocity if nonequilibrium is avoided or minimized. The assumed gas is air and only oxygen dissociation is considered. α_{fo} represents the mass fraction of oxygen dissociation. The method of calculation is that of Bray (Ref. 24) and is based on the approximation of a sudden freezing process in the noxxle.

A way was suggested in Ref. 25 to account for the influence of ambient dissociation of a simple diatomic gas, as might exist in a wind tunnel using nitrogen as the test medium. This method consists of subtracting the ambient degree of dissociation from the free-flight shock-layer dissociation under similar flow conditions. Another scheme advanced to help the experimenter is the binary-scaling method of Ref. 26.

Analysis of nonequilibrium, high-enthalpy flows is complicated by the necessity to take into account simultaneously the many reaction processes and their interdependence. It has been suggested (Ref. 26) that a scaling law for simulation of flows with coupled chemical reactions is represented by the produce $\rho_\infty L$ = const. when U_∞ = const., if all chemical reactions occur through two-body, or binary, collisions, In this case, L represents body scale (e.g., nose radius), ρ_∞ = freestream density, and U_∞ = freestream velocity. This procedure is said to automatically scale the corresponding inviscid, afterbody flows correctly at a given Mach number if either the latter are frozen or else the three-body recombination remains unimportant. Also, the afterbody boundary-layer flow is correctly scaled by the same process if atom diffusion dominates over recombination, correct surface conditions are maintained, and velocity and Mach number are duplicated.

The foregoing examples show the large part of the operating map of aerospace vehicles wherein nonequilibrium, real-gas influences may exist, and the difficulty of duplicating flight conditions in laboratory facilities. The next task is the evaluation of the importance of these matters in the determination of aerodynamic performance of full-scale free-flight vehicles on the basis of laboratory experiments, i.e., is only partial simulation adequate? Fortunately, the answer to this question often is a qualified yes, particularly in regard to rarefied flows, which receive the most attention in this lecture.

SIMULATION OF RAREFIED FLOW FIELDS

It is the purpose of this section to offer some remarks on aerodynamic simulation in the particular case of low-density, hypersonic flows. Considering the scarcity of flight data, one can only partially assess the validity of laboratory data at this time. Quite possibly, we are on the verge of developments which could provide data in abundance. But, in view of the continuing deficiency in detailed full-scale, free-flight results suitable for critical comparison with tunnel and range data, one should not anticipate any such sudden change in circumstances. Comments pertaining to some aspects of the subject follow, but first the present interpretations of the terms "low-density" and "hypersonic" require a few words.

Here, and in other parts of this lecture, "hypersonic" is taken to mean freestream numbers, M_∞, sufficient in regard to any particular problem to approximate closely the conditions of $M_\infty > 20$. It is well known that this requirement may sometimes be met when $M_\infty \approx 4$ and in other cases it is necessary that $M_\infty > 20$. The lecturer wishes to suggest that a reasonable criterion for "low-density" is

$$\lambda \simeq 1.49\, M_\infty/(Re_\infty/\text{ in}) = 0\,(0.02 \text{ in.}).$$

where

λ_∞ = mean free path in freestream

M_∞ = Mach number

R_∞ = Reynolds number

Note that the Knudsen number, $\lambda_\infty/L \sim M_\infty/Re_\infty$.
Other definitions, including those not involving dimensions, may be proposed. However, note that unless a dimension is used in the definition, any wind tunnel may be called a low-density tunnel because of the evident possibility of using very small models to achieve very low Reynolds numbers regardless of test section conditions.

To further examine the low-density criterion advanced here, note that λ_∞ = 0.02 in. when the altitude in the Earth's atmosphere is approximately 220,000 ft. If, at that altitude, the velocity is 20,000 fps, then $Re_\infty \approx$ 20,000/ft and $M_\infty/\sqrt{Re_\infty/ft} \approx 0.14$. Neither blunt nor sharp-nosed, full-scale bodies of typical size will experience pronounced second-order effects of rarefied flow under these conditions, but increasing altitude will bring on rapidly growing effects.

Unfortunately, the suggested criterion is not really as precise as one would wish. The problem is much the same as that of defining hypersonic flow, because a low-density flow need only be as rarefied as the particular experiment requires. It is obvious that, by this standard, only the indivdiual experimenter can decide if his is effectively a low-density flow.

One additional remark concerning the flow regimes should be made. Namely, because almost all cases of practical interest are characterized by the "cold-wall" condition, it is very desirable that low-density wind tunnel tests simulate situations where wall temperature is well below adiabatic recovery temperature.

Real-Gas and Nonequilibrium Effects in Rarefied Flow

Thermo-chemical nonequilibrium more often becomes a factor when low-density conditions exist. But a compensating feature in this connection is that freezing of vibratory and dissociative energies occurs more readily at low densities, making most of the rarefied-flow regimes also essentially perfect-gas regimes. In the latter case, much may be accomplished with wind tunnels and aeroballistic ranges producing approximate Mach and Reynolds number simulation without duplicating stagnation conditions or body dimensions. In particular, pressures, forces, and moments, as well as heat transfer rates, in many cases are little affected by real-gas phenomena. This state of affairs is more understandable when the factors determining heating rates and pressures are reviewed.

Heat Transfer Rate - A very large percentage of the total enthalpy may be represented by a few percent dissociation. Heat transfer rates are determined by the difference between the generalized recovery enthalpy and the thermal enthalpy corresponding to surface temperature. To be more specific, consider the laminar, axisymmetric, stagnation-point, boundary-layer flow discussed by Rosner in Ref. 27, among others. He shows that the heat transfer rate at the stagnation point is:

$$\dot{q} = 0.763 \left(\frac{\rho_w u_w}{\rho_e u_e}\right)^{0.1} (\beta \rho_e u_e)^{0.5} (Pr_{\lambda,f})^{-0.6} \Delta h \left\{ 1 + \phi \left[(Le_f)^{0.6} - 1 \right] \Delta h_{chem,\,eq} / \Delta h \right\}$$

The definitions of particular importance at this point are

$$\Delta h = (h_e - h_{f,w}) - (1 - \phi)\, \Delta h_{\text{chem, eq}}$$

$$\phi = (\alpha_e - \alpha_w) / \alpha_e = \Delta h_{\text{chem}} / \Delta h_{\text{chem, eq}}$$

h_e = total enthalpy at edge of boundary layer, including chemical contributions

$h_{f,w}$ = chemically frozen enthalpy at the wall, i.e., thermal enthalpy based on wall temperature

Δh_{chem} = change in chemical energy content across boundary layer

$\Delta h_{\text{chem, eg}}$ = equilibrium value of Δh_{chem}

It follows that the major influence of chemical processes on $\dot{q}$ is represented by

$$\Delta h = (h_e + h_{\text{chem, e}} - h_{\text{chem, eq,e}}) - (h_{f,w} + h_{\text{chem, w}} - h_{\text{chem, eq, w}})$$

and

$$\Delta h_{\text{chem}} = h_{\text{chem, e}} - h_{\text{chem, w}}$$

In otherwise equivalent cases, if recombination is completed to the same degree and if Δh is equal, these results imply that $\dot{q}$ will be equal regardless of whether recombination occurs in the boundary layer or on the wall.

The importance of surface catalylicity in connection with dissociated freestream flows should not be overlooked. Boundary layers, even at stagnation points, are expected to be essentially frozen

throughout practically all of the low-density regime defined earlier in these remarks, cf Refs. 6 and 27-30, but surface recombination may remain effective. Thus, even if low densities do not permit appreciable vibratory excitation or dissociation behind shock waves, portions or all of any energy content of the freestream related to vibration and dissociation may be transferred to the body surface. Therefore, if such energies are frozen in the expansion of flows from tunnel settling chambers, they must be accounted for in the interpretation of test data.

An example of the effect of frozen dissociation energy in the expanding nozzle flow may be of interest. As an exploratory experiment, W. H. Carden and J. T. Miller, colleagues of the lecturer, have measured the results given in Table 1. These data represent heat transfer rates to hemispherical noses of electrical cooper in a heated, slightly dissociated nitrogen stream. Non-catalytic coatings of orthophosphoric acid were applied to the cooper model as a viscous liquid and allowed to cure in the tunnel flow until a thin, solid coating remained. This was soft enough to be removable by wiping with emery paper. The $\dot{q}$ measured is the heat transfer rate for the entire hemisphere. Lees' distribution (ref. 31) is assumed in conjunction with Fay-Riddell theory (Ref. 32).

Table 1

Heat Transfer Rates in Dissociated Flow Experiment

	Run 1	Run 2
$\frac{\dot{q}_{meas.,\ clean\ surface}}{\dot{q}_{Fay\text{-}Riddell,\ 100\%\ recomb.}}$ =	0.99	0.96
$\frac{\dot{q}_{meas.,\ coated\ surface}}{\dot{q}_{Fay\text{-}Riddell,\ 100\%\ recomb.}}$ =	0.67	0.63
$\frac{\dot{q}_{Fay\text{-}Riddell,\ 0\%\ recomb.}}{\dot{q}_{Fay\text{-}Riddell,\ 100\%\ recomb.}}$ =	0.54	0.54

To see if the heating was reduced by mass transfer from the coating rather than reduced recombination, we conducted the same test at equal total enthalpy, though somewhat lower impact pressure, in a flow known from our measurements to have essentially no dissociation in the nozzle flow. In that case coating the nose had no influence on heat transfer. Thus, we believe mass-transfer effects were negligible after the coating was "cured." Prior to curing, there was a measurable variation of heat transfer rate with time.

We have data from calorimeters which provide the value of total

entalpy and can compute the active or equilibrium enthalpy from known reservoir and nozzle throat conditions and the nitrogen Mollier chart. Normally, the tunnel is operated at higher reservoir pressures and no evidence of dissociated flow in the nozzle exists.

Pressure - It is easily demonstrated that nonequilibrium thermochemical processes will affect pressures and, therefore, forces and moments on aerodynamic bodies. However, evidence of this is hard to find in experimental data, and it is interesting to consider why this is so.

First, regardless of optimistic predictions of performance, most hypersonic wind tunnels are essentially perfect-gas tunnels. Secondly, only a few percent dissociation exists in the flow over slender, sharp bodies in free-flight or tunnel flows. Therefore, the number of places where one may find relatively strong, aerodynamic evidence of dissociation is greatly reduced. One such place would seem to be the stagnation regions of blunt-nosed bodies in flight at high speeds and at altitudes low enough to permit dissociation to occur in the shock layer. However, in the stagnation regions of bodies at hypersonic speeds, pressures are mainly determined by the product $\rho_\infty U_\infty^2$, where ρ_∞ = freestream density and U_∞ = freestream velocity. Thus, presence or absence of dissociation in the shock layer will not greatly affect this pressure.

If the expansion around a blunt body with appreciable dissociation in the stagnation region is a frozen expansion, under suitable conditions

pressures will differ widely from those corresponding to an equilibrium expansion (cf Ref. 30). It appears that this is the model to investigate if one wants to see nonequilibrium effects on pressures. However, based on the definition of low-density flow given earlier, it is implied that blunt-nosed flows with appreciable dissociation in the shock layer are not likely to be a prominent type of low-density flow because, except at the lower part of the altitude range, densities may be too low to enable dissociation to occur in the shock layer. What does occur presumably will remain largely frozen thereafter (cf Refs. 28 and 33).

From the foregoing, it appears that flight under hypersonic, low-desnity conditions should be relatively free of real-gas effects because thermo-chemical processes will most often be frozen. This means that perfect-gas tunnels simulating Mach and Reynolds numbers with cold-wall test conditions are suitable for most work.

Aeroballistic ranges appear to have some utility for investigation of real-gas influences because they offer a means of producing high speeds in low-density gases of known, controlled composition and the binary scaling rule can be applied. The obvious handicap resulting from having no direct, data-transmitting connection to the model and difficulty of launching complex models at high speed, of course, greatly reduces the advantage that would otherwise be gained by use of ranges for study of real-gas effects.

Some Typical Problems of Low-Density Flow

The last section certainly falls short of a complete analysis of nonequilibrium effects, and the present section must be equally incomplete. Insofar as validity of test data or degree of simulation is concerned, if one assumes that necessary molecular speed ratios and Knudsen numbers are achieved, there remain questions such as those concerning molecular speed distribution, gas-surface interactions, and the techniques of accurate measurements in high-speed, possibly non-continuum flows. These topics are sometimes so related that they can be demonstrated in one example. The thermal transpiration phenomenon is somewhat of this nature (see e.g., Ref 34).

Thermomelecular Flow in Tubes - This phenomenon has received relatively little attention in aeronautics. It may become important in such tasks as the measurement of very low pressures by means of a typical setup whereby the orifice at the point where knowledge of the pressure is desired is connected to the measuring instrument by a tube of small diameter. If Knudsen number is sufficiently large and there is an appreciable temperature gradient along the tube, the condition of zero mass flux along the tube does not correspond to equality of pressure along the tube. Thus, the measurement is in error. The most recent research on this subject has been reported by Arney and Bailey (Ref. 34). A typical example of the results of their investigation is given in Fig. 6.

Figure 6 represents a case where pressure at the cold end of a tube is three-fourths the pressure at the hot end when the Knudsen number is 10 and the temperatures differ by a factor of 1.955. In the course of these experiments, four weeks' time was allowed for outgassing the apparatus which was maintained under vacuum at elevated temperature during this period. Approximately $\pm$ 5 percent scatter is indicated by the data at higher Knudsen numbers, but it is noteworthy that this experimental scatter corresponds to only about $\pm$ 0.5 micron Hg. Based on data such as these, charts for use in estimating the thermomolecular flow correction have been prepared (Ref. 33).

Gas Surface Interaction - The lecturer believes that the problems of simulation and measurements in noncontinuum flows go deeper than the mere production of high-speed, very-low-density streams. There are questions related to surface cleanliness which affects accommodation coefficients (Refs. 12 and 35). All tests in wind tunnels thus far involved models with "engineering surfaces" -- a term believed to have been coined by physicists to denote unclean surfaces. It may be added that the origin of the term is no more obscure than the specific definition of such a surface. However, a considerable difference may exist between, say, heat transfer rates to bodies cleansed of all foreign gases and other matter and the usual type of wind tunnel model in noncontinuum flows. Obviously, accommodation coefficient may vary with time of exposure of the surface to low-pressure environment.

Other peculiarities of rarefied flow may be mentioned. For example, at sufficiently high speeds, the recoil forces of ablating body material may be significant. Pressures along the axes of orifices may be variable even in the absence of temperature gradients in the orifice walls if temperature gradients exist in the gas at the orifice entrance. This latter phenomenon is discussed in a recent paper (Ref. 36).

Orifice Effect - A problem may arise when it is attempted to measure pressures on a solid surface in rarefied flow by the usual method involving an orifice in the surface connected to a pressure transducer. The pressure at the surface and that in the orifice cavity will be equal, only if there is no heat or momentum transfer, or other net fluxes to or from the surface at the orifice. By utilizing a two-stream Maxwellian velocity distribution, a relation between measured pressure, p_i, true pressure on the surface, p_{io}, and heat transfer rate, $\dot{q}$, was derived in Ref. 36 for a case where only heat transfer was considered to contribute to the orifice effect. The theoretical analysis was limited to very large Knudsen numbers, i.e.,

$$\lambda_w/d \gg 1$$

where

λ_w = mean free path based on wall temperature

d = Orifice diameter

An experiment was devised to extend the investigation to low Knudsen numbers, thereby enabling the drawing of curves to be used in correcting experimental data. A typical result of applying the data of Ref. 36 is illustrated in Fig. 7.

Several points of interest are apparent in Fig. 7. First, it may be observed that measured static pressures increased roughly 30 percent as orifice size increased in these examples. Further, it is inferred that much larger orifices would be necessary to avoid the orifice effect. Also, the predicted curves are in close agreement with the experimental data.

Nozzle Design - Although it is not the only design problem connected with low-density, hypersonic (LDH) wind tunnels, nozzle design is important and interesting. If we consider that the model LDH tunnel should have heated flow, then there is not only the problem of calculating boundary-layer thicknesses but also that of throat heat transfer rate.

Some high-enthalpy wind tunnels, not necessarily LDH type, incorporate conical nozzles, which are cheaper to build and less sensitive to off-design operating conditions. However, conical nozzles normally have undesirable axial gradients in flow properties through the test section. Such gradients often are not prohibitive if blunt-nosed, short (bluff) bodies are being tested, but appreciable errors may be incurred if slender bodies are tested, cf Ref. 37. Figure 8 taken from Ref. 37, shows an example of the error incurred. More recently, C. H. Lewis of ARO, Inc., has calculated the pressure distribution on cones in both parallel and diverging flow by the method of characteristics. The results of these more refined calculations also indicate large errors when long bodies are tested in conical nozzle flows with axial gradients (Ref. 38).

The method used to design contoured nozzles for the arc-heated, continuous type LDH Tunnel (L) in the von Karman Facility* combines an "inviscid core" calculated by the method of characteristics and a boundary-layer correction whereby the displacement thickness, δ^*, is added to the core radii, r_{ec}, to yield nozzle wall radii. Although it is somewhat surprising that the simple addition of displacement thickness suffices when $\delta^* > r_{ec}$, excellent results have been obtained thus far. Nozzles for Tunnel L look almost conical because of the large boundary-layer corrections, as illustrated in Fig. 9. Calibration results for the nozzle of Fig. 9 have shown that computed and measured displacement thicknesses are in very good agreement. There is no axial gradient in the test section of this nozzle, and radial uniformity in the inviscid core is also excellent.

Pumping Systems - It is not intended to discuss the engineering of pumping systems, although they are of utmost concern in connection with larger LDH tunnels. Rather, the opportunity is taken to emphasize the important benefits of diffusers, which were considered to offer little pressure recovery in low-density flow until it was shown (Ref. 3, pp. 599 - 624 and Ref. 39) that sufficient recovery could be attained to enable large savings in pumping system cost to be realized. Figure 10 illustrates the variation of diffuser efficiency with Reynolds number. Coupling diffusers with use of overexpanded nozzles (Refs. 39 and 40)

---

* von Karman Gas Dynamics Facility (VKF), Arnold Engineering Development Center (AEDC), Air Force Systems Command (AFSC).

allows pressure at the entrance of the pumping system to be 15 to 20 times greater than static pressure in the test section of the nozzle. Dr. Ray Chuan of Celestial Research Corporation has privately communicated to the lecturer the information that cryopumping, i.e., boundary-layer freezing, in diffusers further enhances their performance.

Other problems which arise in work with LDH facilities will be apparent in the following section. Some of these are due to small model size and low aerodynamic loads in existing, pilot facilities.

Some Results from the AEDC - VKF Low-Density Hypersonic Tunnel

To illustrate some of the practical reasons for studying LDH flows, a few results are presented.

Heat Transfer - Total heating rates of various blunt-nosed shapes have been measured in Tunnel L (Ref. 41). Total heat flux (Btu/sec) to the entire nose was measured and converted to average heat transfer rate per unit area by dividing the total heat flux by the wetted area of the nose. Results for the hemispherical shape are shown in Fig. 11. The data in Fig. 11 are normalized by dividing the measured rates by those calculated from a theory for flows corresponding to higher Reynolds numbers. In the calculation, the theory of Fay and Riddell (Ref. 32) was used to obtain heating rate at the stagnation point, and the theory of Lees (Ref. 31) was used to obtain the distribution of heating rates around the hemisphere. The data in Fig. 11 clearly show the effects of reduced Reynolds numbers.

The results of three theories (Refs. 42, 43, and 44) applicable for low Reynolds numbers are shown in Fig. 11 for comparison. Qualitative agreement is evident, but some difference in actual values exists. It should be noted that the theories only yield the stagnation-point heating rate. Lees' distribution was assumed in converting these theoretical, stagnation-point values to average values. Thus, the comparison is possibly slightly qualitative for that reason. There are data for low Reynolds numbers showing Lees' distribution to be close to the experimental.

Drag - Both sharp- and blunt-nosed cones have been tested to determine drag under low-desnity conditions. A water-cooled, sting-type balance capable of resolving drag forces on the order of 0.001 lb was used. The marked effects of combined low Reynolds number and high Mach number are illustrated by the data presented in Fig. 12. It may be seen there that the drag coefficient at $M_\infty/\sqrt{Re_\infty} \approx 0.3$ is roughly three times the value when $M_\infty/\sqrt{Re_\infty} \approx 0$ for the more bluff body and 12 times greater for the more slender body. For a 15-ft body at orbital velocity, this condition of $M_\infty/\sqrt{Re_\infty} \approx 0.3$ would exist at approximately 300,000-ft altitude. More slender bodies, such as delta wings, tested in Tunnel L have yielded drag coefficients nearly 20 times greater than their essentially inviscid values.

Through use of the low-density, hypersonic wind tunnel of the von Karman Gas Dynamics Facility, drag of spheres has been measured under hypersonic, cold-wall, support-free conditions in a nonreacting flow in which molecular vibration was frozen (Ref. 45). Data were obtained

for a nominal freestream Mach number of 11 and for Reynolds numbers from 1 to 10 based on conditions immediately downstream of an assumed Rankine-Hugoniot type of normal shock and sphere diameter. Photographs were taken of the tracks of small spheres falling through the test section of Tunnel L and being deflected by the drag force, which was calculated by knowledge of the mass of the sphere, time interval, and distance between the images on the photo. These data were supplemented by measurements at a nominal Mach number of 10 where a conventional balance was used, and Reynolds numbers downstream of the shock as high as 10^4 were investigated in the cold-wall condition.

The experimental results have been analyzed both from the point of view of continuum flow with second-order viscous effects and from the standpoint of a noncontinuum concept, taking account of first collisions between re-emitted and freestream molecules. Results are shown in Fig. 13.

Shock Waves - An experimental investigation has been made to determine the pressure distribution, shock shape, detachment distance, and wave thickness for spheres, and the latter three characteristics for flat-bodies in heated argon where Mach number was from 4 to 14, stagnation temperature was from 1900 to 4100°K, and Reynolds number downstream of the normal shock waves was 25 to 225 based on radius (Ref. 46). The purposes of this investigation were to determine the validity of the various theories available for predicting the above properties in the low- flow regime and to extend available data to lower Reynolds numbers.

When argon is used as the working gas, at the nozzle exit and some distance downstream there is a clearly visible, light-blue jet surrounded in most cases by a pink glow. This natural glow, thought to be caused by radiation from relaxing metastable atoms, enabled this study of the shock properties in front of spheres and flat-faced bodies to be made by simply photographing the flow field, wherein the brightness was proportional to the number density of radiating atoms.

Photographs of the shocks generated by the spheres and flat-faced bodies were analyzed with a photo-densitometer to determine the shock shape, detachment distance, and wave thickness.

In Fig. 14 the results of the measurement of shock detachment distance for spheres at different wall-to-stagnation temperature ratios is shown. It will be noted that the shock detachment distance is a function of Mach number, Reynolds number, wall temperature, and body shape. A study of the magnitude of the shock-wave and boundary-layer thicknesses indicates that in these tests these layers were incipiently or fully merged. As the Reynolds number decreases, the shock detachment distance increases to values more than double the "inviscid" values. Also, for the bodies where the wall-to-stagnation temperature ratio is 0.1, there is evidence to confirm the decrease in shock detachment distance to a value less than the inviscid value, as predicted by Ho and Probstein (Ref. 47), before the increase as mentioned above for the lower Reynolds numbers.

Three-Component Measurements - The effect of rarefied flow on drag of representative bodies has been illustrated in Figs. 12 and 13. Other

aerodynamic forces and moments also are affected, and it is desirable to determine these on the basis of experiments because the theoretical computation is not yet sufficiently reliable.

Figure 15 relates the viscous interaction parameter, $M_\infty \sqrt{C_\infty / Re_\infty}$, to vehicle size and altitude above Earth for a typical gliding atmospheric entry trajectory from orbital or lunar excursions. At altitudes of roughly 300,000 ft, forces may be roughly 1/50 their values at 200,000 ft, but considerations of stability and lift-to-drag ratios are none the less important in some cases. Therefore, designers have need for aerodynamic data of the type forthcoming from more common wind tunnel tests. To explore the problem and with the hope of gaining a capability for measuring lift, drag, and pitching moment, colleagues of the author have developed the balance described in Ref. 48. A photograph of this remarkable device is shown in Fig, 16, and a sample of data obtained from a short, blunt conical model is shown in Fig. 17. This model is of interest as a possible Mars probe or Earth satellite. Because the forces and moment measured are more indicative of the balance performance, Fig. 17 gives those data instead of the usual coefficients. In this experiment, based on matching Reynolds numbers, n altitude of 316,000 ft. was simulated under hypersonic, cold-wall conditions.

Viscous Interaction - The hotshot and shock tunnel, impulse-type wind tunnels, and the continuous-type, LDH Tunnel L have been used to investigate pressure distribution on sharp-edged flat plates under

conditions of pronounced viscous interaction. Examples of data from the VKF hotshot and LDH tunnels, as well as data from other sources soon will be published by J. D. Whitfield and H. E. Deskins, ARO, Inc. A preliminary example is shown in Fig. 18. It may be noted that these data, which extend into the region of appreciable slip flow, did not display such relatively good agreement until the method of Ref. 36 was applied to correct for orifice effect. This correction removed discrepancies of up to 45 percent in pressure coefficients.

SIMULATING CONDITIONS OF HIGH REYNOLDS NUMBERS

Much less is included in this section than in the preceding ones which concerned phenomena and simulation problems related to low Reynolds numbers. Really serious efforts to produce large Reynolds numbers under hypersonic conditions seem to have taken second place, in most laboratories, to efforts toward higher Mach numbers and velocities. Lately some indications of renewed interest in facilities providing high Reynolds numbers have seen manifest. Special tests in impulse-type tunnels recently have been arranged so that high Mach number is sacrificed in return for higher Reynolds number. However, the higher Reynolds numbers have been achieved with $5<M_\infty<15$, so the Mach numbers are comparable to large continuous-type tunnels where $M_\infty \leq 10$ and typical maximum $Re_\infty/in. \approx 2 \times 10^5$. Figure 19 represents an attempt to summarize the current Reynolds and Mach number relationship with regard to hypersonic wind tunnels using air or nitrogen gases. The tunnel described by Perry (Ref. 16, pp. 395-422) is said to be

capable of Re_∞/in. = 1.5 x 10^5 at M_∞ = 18 for run times of two to perhaps ten milliseconds. On rare occasions hotshot-type tunnels have produced Re_∞/in. = 0.85 x 10^5 at M_∞=19.

Viewing Fig. 20 and comparing the typical trajectories shown in Fig. 2, it is evident that very high Reynolds numbers may characterize flows on relatively low-drag, heavy bodies during important portions of their descent. For example, a body moving at 18,000 fps at 100,000 ft altitude has a freestream unit Reynolds number of 1.6 x 10^5 per in. Corresponding, Mach and Reynolds numbers attained at the edge of the boundary layer on a 10-deg half-angle cone would be approximately 9.2 and 3.6 x 10^5 per in., respectively. These two cone surface flow conditions are not impossible to simulate in present laboratory facilities but it is necessary to examine the other requirements for natural boundary-layer transition and turbulent flow under the influence of factors present in high-speed flight. For example, the ratio of wall temperature to adiabatic recovery temperature, T_w/T_{aw}, usually is considered a significant parameter in such studies, and, in the free-flight example cited, it would be approximately 0.1. However, by far the largest obstacle to creating these conditions in a wind tunnel exists because of the tendency for Reynolds number of boundary-layer transition, Re_t, to increase markedly as Mach number increases, whether $T_w << T_{aw}$ or not. For the case $T_w \approx T_{aw}$, this is shown by Fig. 21, which is taken from Ref. 50. Supporting data from various sources may be seen in Ref. 51. Actually, comparisons of this type are highly qualitative, for reasons too numerous to discuss here (see, e.g., Refs. 52 and 53), but Fig. 21

serves present purposes. Data, for the case $T_w << T_{aw}$ are less plentiful, but Ref. 51 provides an indication that the ratio T_w/T_{aw} may not be an extremely important factor when local Mach number exceeds, say 5 or 6. In the absence of more plentiful data for the hypersonic case, the latter may be regarded as a conservative assumption in the present context, i.e., Re_t for a cooled wall normally exceeds Re_t for an adiabatic wall. Then, returning to Fig. 21 and assuming Re_t to represent the "end" of transition, one would estimate that $Re_t > 5 \times 10^7$ under conditions described earlier for the sharp cone.* Therefore, using the value of unit Reynolds number of 3.6×10^5 in.$^{-1}$, the distance from the apex of the cone to the end of transition, i.e., fully developed turbulent boundary-layer flow would be at least 140 in. or nearly 12 ft. Few hypersonic wind tunnels are large enough to accept such a large model. From Fig 21, note that transition would begin at about one-seventh of this length or a little less than 2 ft from the nose of the cone. Thus, nearly the entire cone would be covered by a transitional boundary layer. As pointed out in Ref. 54, this is typical of hypersonic flows and it adds to the experimenter's woes. To quickly understand some of the reasons why it is difficult to build wind tunnels which simultaneously produce high Mach and Reynolds number conditions, a few of the problems are briefly outlined.

---

* In Refs. 50 and 54 it is shown that Re_t on a sharp cone at $M_\infty \approx 3$ is more nearly 3 times the value of Re_t on a flat plate or hollow cylinder. However, this factor has not been considered here, partly because its omission is consistent with the estimate of a lower possible value of Re_t and partly because it is not certain that it applies under the conditions being discussed.

Mach and Reynolds numbers in the nozzle of a tunnel are related to reservoir pressure, p_o, and temperature, T_o, such that, for fixed reservoir conditions, increasing M_∞ lowers Re_∞. Fox fixed p_o and M_∞, increasing T_o lowers Re_∞. Now the minimum T_o is established by the need to avoid liquefaction of the gas medium when it expands to low temperature and high M_∞. For a perfect gas, the static temperature at M_∞ is

$$T_\infty = T_o / [1 + (\gamma-1) M_\infty^2/2]$$

where γ= ratio of specific heats

Thus, when $M_\infty >> 1$, $T_\infty \sim T_o/M_\infty^2$, and it is evident that high M_∞ requires high T_o if T_∞ is not to fall below the liquefaction line. Recently there seems to be growing acceptance of the feasibility of allowing T_∞ to be well below the conventional limit, as indicated in Fig. 22 from Ref. 16, p. 335. In other words, the liquefaction rate seems slow enough to effectively displace the change-of-phase boundary in hypersonic nozzle flows. Nevertheless, the requirement to avoid liquefaction presents an obstacle to the combining of high reservoir pressures with low reservoir temperatures to achieve a higher Reynolds number at a given Mach number. Of course, it also should be noted that the throat heat transfer problem influences the relation between p_o and T_o, and the lack of adequate data on viscosity and other properties of air at low temperatures discourages acceptance of very low T_∞ for aerodynamic work.

The hypersonic wind tunnel using helium as the working fluid has

been developed because the low liquefaction temperature of helium largely remove the liquefaction barrier just discussed. (See, e.g., the paper by Henderson in Ref. 1, pp. 163-190.) However, the fluid properties are considerably different from air, making it questionable if inviscid and viscous fluid flow effects can be simulated simultaneously when using helium to test configurations with complicated flow fields involving strong shocks, separated flows, and shock-boundary layer interference. Simpler measurements of, say, friction drag on slender, sharp-nosed bodies may be carried out with air closely simulated.

Aeroballistic ranges wherein a model may be launched at very high velocity into relatively dense air offer possibilities for study of boundary-layer transition under hypersonic, cold-wall conditions. (See, e.g., the paper by Charters and Curtis in Ref. 1, pp. 371-404, and Refs. 55 and 56). The range is attractive because of high attainable Reynolds numbers (see Fig. 19), low ambient air turbulence, the possibility to achieve high Mach numbers, and the cold-wall condition of the model. Disadvantages are rather obvious, e.g., the model may pitch and yaw, optical methods must be relied on for transition detection, under some conditions the model may ablate, and it is difficult to launch and separate sabots from complex models. The range is almost essential for studies of wakes far downstream of bodies, regardless of Reynolds numbers of interest.

Counterflow, range-plus-tunnel, facilities offer some of the same advantages as ranges, but they also suffer most of the same disadvantages as the range in addition to those pertaining to impulse-type

tunnels. Very high relative velocities have been proved feasible and unit Reynolds numbers up to 5×10^6 in $^{-1}$ at 35,000 fps are attainable according to Ref. 57. Seiff, in Ref. 57, suggests that relative velocities as high as 50,000 to 60,000 fps may be reached in the next five years. This performance is an indication of the reason why counterflow facilities are intersting.

PLANETARY ATMOSPHERES

Because of contemplated exploration of other planets, aerodynamic simulation of the atmospheres of these planets has become a concern of the aerodynamicist. Some studies of lift, drag, and stability have been accomplished, e.g., Refs. 58-60. In Ref. 58, a blunt-nosed, axisymmetric cylinder with a flared afterbody is shown to yield different static-stability derivatives in different, unmixed gases, the static stability increasing as ratio of specific heats, γ, increases. One infers from these data that γ is the dominant variable, because it appears that the results were the same in argon and helium.

Reference 60 reports tesys of two blunt, conical bodies in air and in gases composed of varying amounts of nitrogen and carbon dioxide, mixed to simulate atmospheres of Mars and Venus. Both a very blunt cone of 10-deg half-angle and a moderately blunt(nose radius = 0.5 base radius) cone of 15-deg half-angle were tested. It was concluded that drag coefficients of these bodies were not perceptibly affected, even when comparing data where N_2>97% with data where CO_2>78%. The very bluff body experienced a slight decrease in stability in the

medium with the percentage of CO_2 large ($\approx$85%), i.e., the trend was in qualitative agreement with results of Ref. 58 described above. However, the moderately blunt cone appeared to become slightly more stable in the case where CO_2 was the major constituent (>78%). Stability of both models seemed little different when CO_2 = 14% and N_2 = 86% and when N_2>97% or when the gas was air. Seiff (Ref. 4, p. 29) has suggested that configurations which generate embedded flow fields (i.e., fields containing secondary shock waves) are more sensitive to gas composition.

CLOSING REMARKS

Although not intending to undertake to catalog all known means for hypersonic aerodynamic simulation, the lecturer wishes to close this discussion with a few remarks on certain particularly relevant types of facilities. In doing this, examples are drawn from the AEDC-VKF complex.

Continuous - or Intermittent-Type Wind Tunnel

The continuous-or intermittent-type hypersonic tunnel employing a resistance-type electric heater or a storage heater and capable of $8<M_\infty<14$ must be accorded a full share of the credit forour present knowledge of hypersonic aerodynamics. A good representative of this class is AEDC-VKF Tunnel C, shown in Fig. 23. Capable of M_∞ = 10 (later 12) and having a 50-in.-diam. test section, this tunnel has

been used in the development of almost every aerospace system involving hypersonic aerodynamics. One of the noteworthy features of this tunnel is its "bomb bay" doors opening from the test section to a cabin below. The model support system withdraws the model into this cabin for cooling and/or adjustments while the tunnel compressor plant continues to run. At the chosen time, the model and its supports are injected into the tunnel flow. This method has proved very advantageous for measurements of heating rates, data being obtained more rapidly and economically. Further description may be found in Ref. 61.

Impulse-Type, High-Enthalpy Wind Tunnel

The large, impulse-type tunnel of either the shock tunnel or hotshot variety also has provided a major share of the support of hypersonic flight. Typically these are operated with $M_\infty \simeq 20$ and with total temperatures which place them in the border region of perfect-gas and real-gas regimes. Hotshot-type Tunnel F of the AEDC is shown in Fig. 24 as a representative of this class. Numerous tests have been conducted in connection with the development of aerospace vehicles and also research on fluid mechanics. Papers by Lukasiewicz, Whitfield, and Jackson in Ref. 3, pp. 473-511, and Ref. 1, pp. 323-356, give further information on the hotshot type of wind tunnel. At the present time, studies of advanced shock tunnel designs are being conducted because of the apparent potential for improved performance offered by the shock-heating process. Consideration is being given to the augmentation of the shock tunnel driver by magnetogasdynamic acceleration.

Low-Density, Hypersonic (LDH) Wind Tunnel

A major part of this lecture is devoted to descriptions of low-density flow research. While the wind tunnel used for this work cannot be called typical, it is, none the less, mentioned here because of its prominent role in aerodynamic studies of LDH flows. The present AEDC Tunnel L, now four years old, is quite small. Typically, the usable, uniform core of flow in the test section is 1- to 2-in. diam. However, experience with this little, prototype facility once again teaches us how much can be learned from such a modest monetary investment.

Because this type of tunnel is not yet widely represented in the world's laboratories but is beginning to appear in increasing numbers, a sketch showing the main features of an idealized, typical LDH tunnel is included as Fig. 25. It should be pointed out that various arc-heated tunnels were used for heating studies preceding the advent of the LDH-type "aerodynamic" wind tunnel. Flow quality and calibration procedures were not of so much concern in these earlier facilities, but high enthalpy was the main concern. For aerodynamic work, the potential of the arc heater for high enthalpy has been subordinated to achieve more steady, uniform flow of lower total enthalpy closer to thermochemical equilibrium. Figure 26 is a photograph of AEDC-VKF Tunnel L. More details may be found in Ref. 62. The possibility of combining magnetogasdynamic acceleration with arc-heated tunnels is receiving serious consideration at several laboratories.

Aeroballistic Range and Counterflow Facility

These two types of experimental facilities are related to such an extent that both are combined in the few remarks made here. To better illustrate each type, Fig. 27 is included. The very great length of these facilities makes it difficult to obtain photographs clearly showing their main features. Figure 27 is divided into three parts, the top part showing a shock tube, the middle showing nozzle, test section and dump tanks, and the lower part showing a launcher or gun. Combining the top two components of Fig. 27 gives a shock tunnel. Combining the bottom component with the middle part, excluding the nozzle, gives an aeroballistic range. Putting all together, of course, yields the counterflow facility.

Although very high muzzle velocities may be produced by modern aeroballistic launchers, the peak launch accelerations (up to 10^6 - 10^7 g's) are so great that model and sabot structural problems arise. In fact, if it were not for this obstacle, we might be telemetering aerodynamic data from models in flight. Figure 28 is offered as a summary of the current ability to launch models in ranges. Areas to the lower left of the three boundaries represent achieved launches. One can see why the aeroballistic range or the combined shock tunnel and gun is attractive to aerodynamicists seeking closer simulation of orbital and super-orbital flight. Practical problems of great difficulty also are apparent, but further development seems to be worthwhile. Figures 29a and 29b show gun and shock tunnel components of the pilot counterflow facility at AEDC-VKF. References pertaining to

these devices have been mentioned earlier, e.g., Refs. 1, 15, 16, 56, and 57. One may also find more information on guns in Refs. 63-65.

Various, less-well-developed but interesting types of facilities could be mentioned, e.g., expansion tubes, high intensity molecular beams, and any of several devices wherein acceleration of ionized gases plays a key role. However, these latter are still in developmental stages and have not yet played important parts in aerodynamic simulation work. Free-flight research using rocket booster models may be regarded as simulation in a broader sense, but it is beyond the scope of this discussion. It is understood that a later lecture will deal with this subject.

ACKNOWLEDGMENTS

The lecturer owes thanks to all of his colleagues in ARO, Inc., and the Arnold Engineering Development Center, Air Force Systems Command, USAF, for their cooperation during the preparation of this material. In addition to those employes of ARO cited in the references, particular acknowledgments are due G. W. Chumbley and Mrs. Maxine O'Dear.

REFERENCES

1. The High Temperature Aspects of Hypersonic Flow. (W. C. Nelson, ed.) Pergamon Press, Oxford, London, New York and Paris, 1964.

2. Reentry Dynamics, Proceedings of the Conference on Physics of the Solar System and Reentry Dynamics. Bulletin of the Virginia Polytechnic Institute, Engr. Exp. Sta. Series No. 150, Vol. LV, No. 10, August 1962.

3. Hypersonic Flow Research. (F. R. Riddell, ed.) Academic Press, New York and London, 1962.

4. Proceedings of the NASA - University Conference on Science and Technology of Space Exploration: Aerodynamics of Space Vehicles (NASA SP-23) and Gas Dynamics in Space Exploration (NASA SP-24). Chicago, December 1962.

5. "Aerospace Engineering: High Temperatures Issue." Aerospace Engineering, Vol. 22, No. 1, Institute of the Aerospace Sciences, January 1963.

6. Cheng, H. K. "Recent Advances in Hypersonic Flow Research." AIAA Jour., Vol. 1, No. 2, pp. 295-310, February 1963.

7. Symposium on Dynamics of Manned Lifting Planetary Entry. (S. M. Scala, A. C. Harrison and M. Rogers, eds.) John Wiley and Sons, New York and London, 1963.

8. Eggers, A. J. and Wong, T. J. "Motion and Heating of Lifting Vehicles During Atmosphere Entry." Paper presented at ARS Conference on Lifting Reentry Vehicles, April 4-6, 1961, in Palm Springs, California

9. "Physics of Entry into Planetary Atmospheres." AIAA Conference Cambridge, Massachusetts, Preprints 63-433 to 63-465, August 26-28, 1963.

10. "International Symposium on Fundamental Phenomena in Hypersonic Flow." Sponsored by Cornell Aeronautical Laboratory, Inc., June 25-26, 1964. Proceedings to be published by Cornell University Press.

11.- Rarefied Gas Dynamics. (Ed. by F. M. Devienne, 1959, Ref.
14. 11; L. Talbot, 1961, Ref. 12; J. A. Laurmann, 1964, Ref. 13; and J. H. deLeeuw, 1965, Ref. 14, to be published.) Academic Press, New York and London.

15. Advances in Hypervelocity Techniques: Proceedings of the Second Symposium on Hypervelocity Techniques. (A. M. Krill, ed) Plenum Press, New York, 1962.

16. Advanced Experimental Techniques for Study of Hypervelocity Flight: Third Hypervelocity Techniques Symposium. Co-sponsored by Denver Research Institute, University of Denver, and Arnold Engineering Development Center, ARO, Inc., 1964.

17. Hall, J. G. "Studies of Chemical Non-equilibrium in Hypersonic Nozzle Flows." Cornell Aero. Lab. Rept. 1118-A-6; AD 229131, November, 1959.

18. Ferri, A., "Hypersonic Flight Testing." International Science and Technology, No. 28, April 1964.

19. Henshall, B. D. "A Review of the Development of High Enthalpy Aerodynamic Test Facilities." Appl. Mech. Rev., Vol. 13, No. 6, June 1960

20. Lordi, J. A. and Mates, R. E. "Nonequilibrium Expansions of High-Enthalpy Airflows." Cornell Aero. Lab. Rept. No. AD-1716-A-3, March 1964.

21. Hurle, I. R., Russo, A. L. and Hall, J. G. "Spectroscopic Studies of Vibrational Nonequilibrium in Supersonic Nozzle Flows." Jour. of Chem. Physics, Vol. 40, No. 8, pp. 2076-2089, April 15, 1964

22. Potter, J. L., Arney, G. D., Jr., Kinslow, M., and Carden, W. H. "Gasdynamic Diagnosis of High-Speed Flows Expanded from Plasma States." IEEE International Symposium on Plasma Phenomena and Measurements, San Diego, California, October 29 - November 1, 1963.

23. Potter, J. L., Arney, G. D., Jr., Kinslow, M., and Carden, W. H. "Irreversible Flow in Reservoir and Throat Sections of Wind Tunnels with Constricted-Arc Heaters." Paper to be presented at AGARD Fluid Dynamics Panel Specialists Meeting, Rhode-Saint-Genese, Belgium, September 21-23, 1964.

24. Bray, K. N. C. "A Sudden-Freezing Analysis for Non-equilibrium Nozzle Flows." University of Southampton, AASU Rept. No. 161, December 1960.

25. Gibson, W. "The Effect of Ambient Dissociation and Species Diffusion on Non-equilibrium Shock Layers." Paper 63-70, presented at the 31st Annual IAS Meeting, New York, January 1963.

26. Hall, J. G., Eschenroeder, A. Q., and Marrone, P. V. "Blunt-nose Inviscid Airflows with Coupled Nenequilibrium Processes." J. Aerospace Sci., Vol. 29, No.9, September 1962, pp. 1038-1051.

27. Rosner, D. E. "Scale Effects and Correlations in Nonequilibrium Convective Heat Transfer." AIAA J., Vol. 1, No. 7, July 1963, pp. 1550-1555.

28. Chung, P. M. "Hypersonic Viscous Shock Layer of Nonequlibrium Dissociating Gas." NASA TR R-109, 1961.

29. Inger, G. R. "Nonequilibrium Hypersonic Flat-Plate Boundary-Layer Flow with a Strong Induced Pressure Field," AIAA J., Vol. 2, No. 3, March 1964, pp. 452-460.

30. Whalen, R. J. "Viscous and Inviscid Nonequilibrium Gas Flows." J. Aerospace Sci., Vol. 29, No. 10, October 1962, pp. 1222-1237.

31. Lees, L. "Laminar Heat Transfer over Blunt-Nosed Bodies at Hypersonic Flight Speeds." Jet Propulsion, Vol. 26, No. 4, April 1956, pp. 259-269.

32. Fay, J. A. and Riddell, F. R. "Theory of Stagnation Point Heat Transfer in Dissociated Air." Jour. of the Aero/Space Sciences, Vol. 25, No. 2, February 1958, pp. 73-85.

33. Talbot, L. "Survey of the Shock Structure Problem." ARS Jour., Vol. 32, No. 7, July 1962, pp. 1009-1016.

34. Arney, G. D. and Bailey, A. B. "The Effect of Temperature on Pressure Measurements." AIAA J., Vol. 1. No. 12, December 1963, pp. 2863-2864.

35. Wachman, H. Y. "The Thermal Accommodation Coefficient: A Critical Survey." ARS Jour., Vol 32, No. 1, January 1962, pp. 2-12.

36. Potter, J. L., Kinslow, M. and Boylan, D. E. "Influence of the Orifice on Measured Pressures in Rarefied Flow." Paper presented at the Fourth International Symposium on Rarefied Gas Dynamics, Toronto, 1964.

37. Whitfield, J. D. and Norfleet, G. D. "Source Flow Effects in Conical Hypervelocity Nozzles." AEDC-TDR-62-116, June 1962.

38. Lewis, C. H. Personal communication, July 1964.

39. Boylan, D. E. "An Experimental Study of Diffusers in an Open-Jet, Low-Density, Hypersonic Wind Tunnel." AEDC-TDR-64-47, April 1964.

40. Potter, J. L. and Boylan, D. E. "Experience with an Over-expanded Nozzle in a Low-Density, Hypervelocity Wind Tunnel." AEDC-TDR-62-85, April 1962.

41. Potter, J. L. and Miller, J. T. "Total Heating Load on Blunt, Axisymmetric Bodies in Low-Density Flow." AIAA Journal, Vol. 1, No. 2, February 1963, pp. 480-481.

42. Cheng, H. K. "Hypersonic Shock-Layer Theory of the Stagnation Region at Low Reynolds Number." Cornell Aero. Lab. Rept. No. AF-1285-A-7, April 1961.

43. Probstein, R. F. and Kemp, N. H. "Viscous Aerodynamic Characteristics in Hypersonic Rarefied Gas Flow." Journal of the Aero/Space Sciences, Vol. 27, No. 3, March 1960, pp. 174-192.

44. Van Dyke, M. "Second-Order Compressible Boundary-Layer Theory With Application to Blunt Bodies in Hypersonic Flow." AFOSR-TN-61, July 1961.

45. Kinslow, M. and Potter, J. L. "The Drag of Spheres in Rarefied, Hypervelocity Flow." AEDC-TDR-62-205, December 1962; AIAA Journal, Vol. 1, No. 11, November 1963, pp. 2467-2473.

46. Bailey, A. B. and Sims, W. H. "The Shock Shape and Shock Detachment Distance for Spheres and Flat-Faced Bodies in Low-Density, Hypervelocity Argon Flow." AEDC-TDR-63-21, January 1963

47. Ho, Hung-Ta and Probstein, R. F. "The Compressible Viscous Layer in Rarefied Hypersonic Flow." Brown University, ARL-TN-60-132, August 1960.

48. Arney, G. D., Jr., and Harter, W. T. "A Low-Load, 3-Component Force Balance for Measurements in a Low-Density Wind Tunnel." IEEE First International Congress on Instrumentation in Aero-Space Simulation Facilities, Paris, September 28-29, 1964.

49. Moore, F. K. "On Local Flat Plate Similarity intthe Hypersonic Boundary Layer." Vol. 28, No. 10, October 1961, pp. 753-762.

50. Potter, J. L. and Whitefield, J. D. "Effects of Slight Nose Bluntness and Roughness on Boundary-Layer Transition in Supersonic Flows." Jour. Fluid Mech., Vol. 12, Part 4, pp. 501-535, 1962.

51. Nagamatsu, H. T. and Sheer, R. E., Jr., "Boundary-Layer Transition on a Highly Cooled 10 deg Cone in Hypersonic Flows." General Electric Res. Lab. Rept. No. 64-RL-(3622C), March 1964.

52. Potter, J. L. and Whitfield, J. D. "Transition Measurements and the Correlation of Transition Sensitive Data." AEDC-TR-59-4, February 1959.

53. Laufer, J. and Verbalovich, T. "Stability and Transition of a Supersonic Boundary Layer." Jour. Fluid Mech. Vol. 9, Part 2, October 1960, pp. 257-299.

54. Potter, J. L. and Whitfield, J. D. "Effects of Unit Reynolds Number, Nose Bluntness, and Roughness on Boundary Layer Transition. AEDC-TR-60-5, March 1960.

55. Lyons, W. C., Jr., Brady, J. J. and Levensteins, Z. J. "Hypersonic Drag, Stability, and Wake Data for Cones and Spheres." AIAA Aerospace Sci. Meeting. Preprint No. 64-44, New York, January 20-22, 1964.

56. Lyons, W. C., Jr., "Application of the Ballistics Range for the Study of Aerodynamic Flow Phenomena About Free-Flight Bodies." AIAA Aerodynamic Testing Conference, Washington, D. C., March 9-10, 1964, pp. 225-238.

57. Seiff, A. "Ames Hypervelocity Free-Flight Research." Astronautics and Aerospace Engr., Vol. 1, No. 1, pp. 16-23, 1963.

58. James, C. S. and Smith, W. G. "Experimental Studies of Static Stability and Radiative Heating Associated with Mars and Venus Entry." Presented at IAS 31st Annual Meeting, New York, January 21-23, 1963.

59. Smith, W. G. and Peterson, W. P. "Free-Flight Measurements of Drag and Stability of a Blunt-Nosed Cylinder With a Flared After-Body in Air and Carbon Dioxide." NASA TM X-642, 1961.

60. Jaffe, P. "Hypersonic Ballistic Range Results of Two Planetary Entry Configurations in Air and Carbon Dioxide/Nitrogen Mixtures." Jet Propulsion Lab. Tech Rept No. 32-543, January 31, 1964.

61. Sivells, J. C. "Aerodynamic Design and Calibration of the VKF 50 in. Hypersonic Wind Tunnels." AEDC-TDR-62-230, March 1963.

62. Potter, J. L. "Low-Density, Hypersonic (LDH) Wind Tunnel L." von Karman Gas Dynamics Facility Technical Developments (J. Lukasiewicz, Ed.) 1964, pp. 61-63.

63. Stephenson, W. B. and Anderson, D. E. "Two-Stage, Light-Gas Model Launchers." Aerospace Engr., Vol. 21, No. 8, pp. 64ff., August 1962.

64. Charters, A. C. and Curtis, J. S. "How an Accelerated Reservoir Light-Gas Gun is Used in a Hypervelocity Free Flight Range." The Jour. of the Environmental Sci., December 1963, pp. 27-32.

65. Curtis, J. S. "An Accelerated Reservoir Light-Gas Gun." NASA TN D-1144, February 1962.

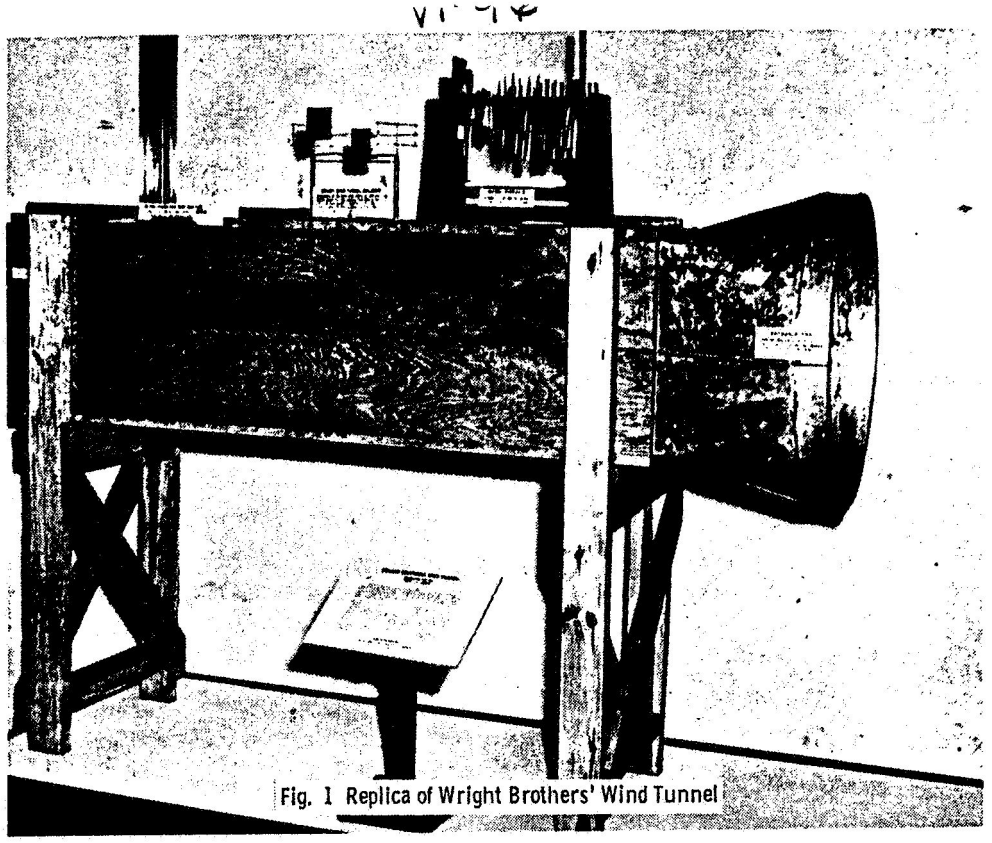

Fig. 1 Replica of Wright Brothers' Wind Tunnel

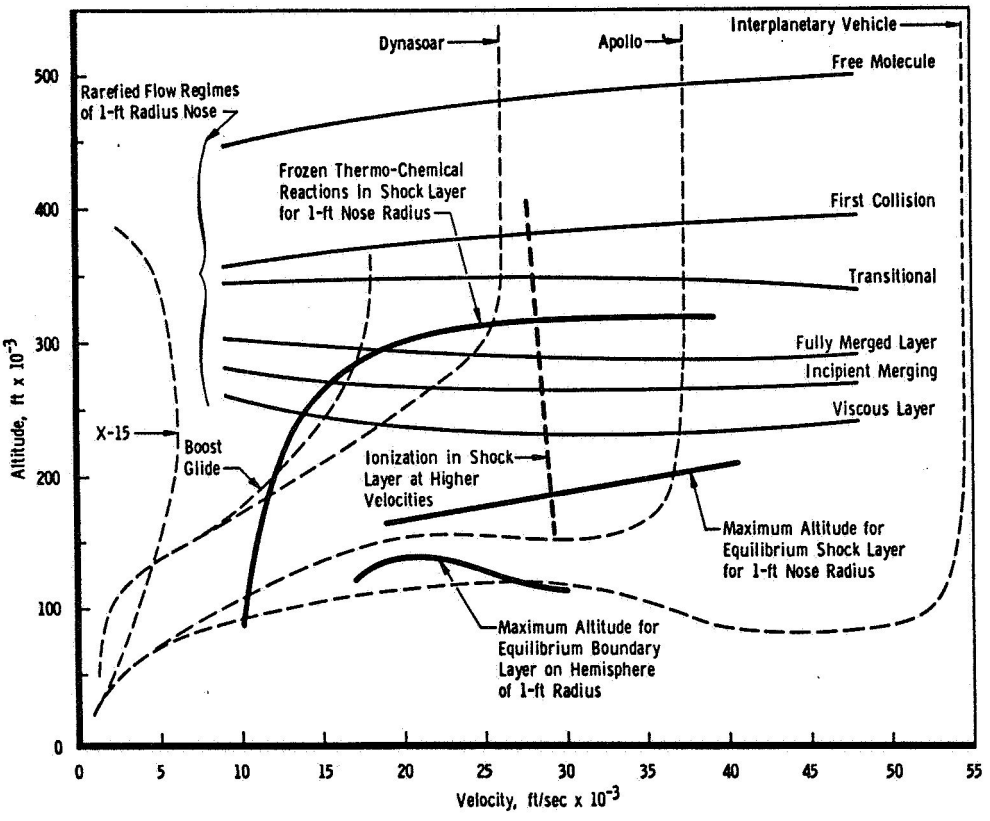

Fig. 2 Flow Regimes and Typical Trajectories in the Earth's Atmosphere (flow regimes apply to the stagnation region of a sphere of 1-ft radius.)

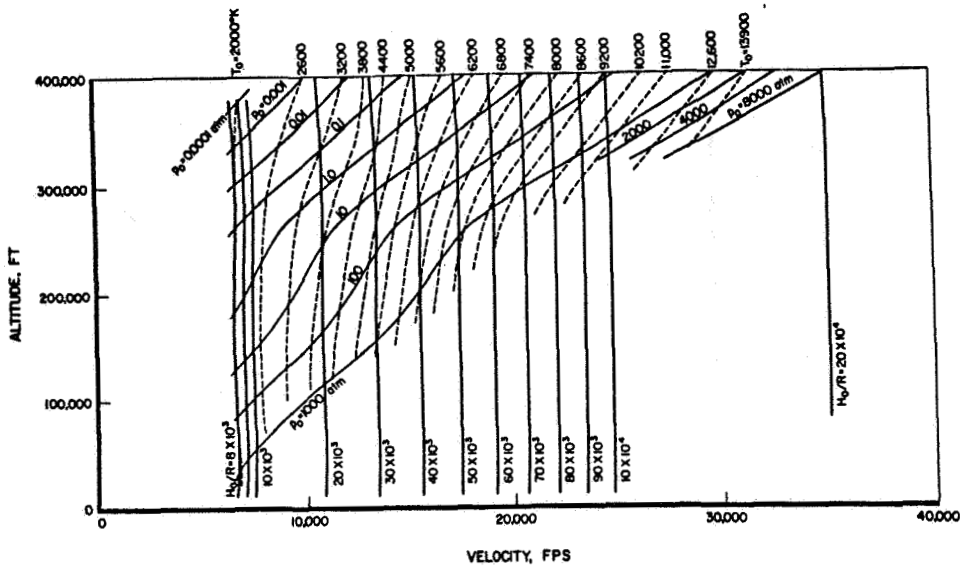

FIG 3 WIND TUNNEL RESERVOIR CONDITIONS CORRESPONDING TO FLIGHT IN THE EARTH'S ATMOSPHERE

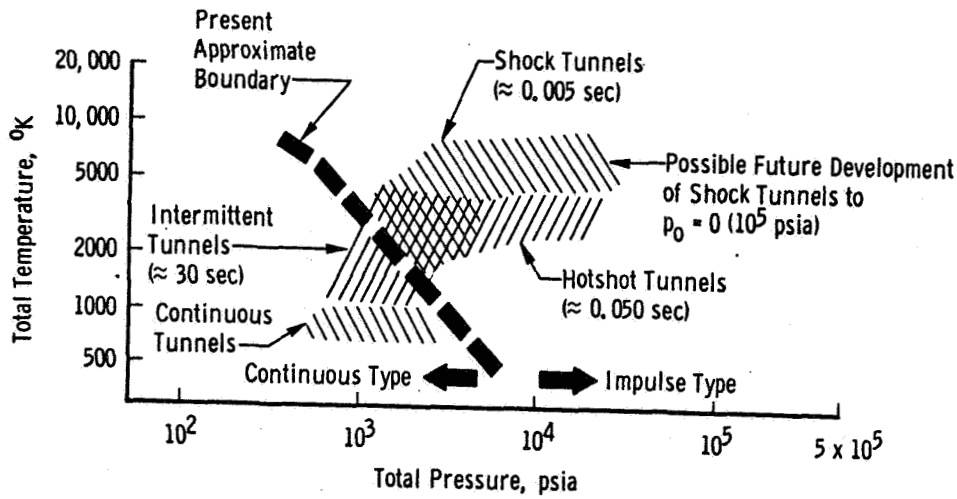

Fig. 4 Approximate Limits Imposed on Conventional Wind Tunnels by Throat Heating Alone

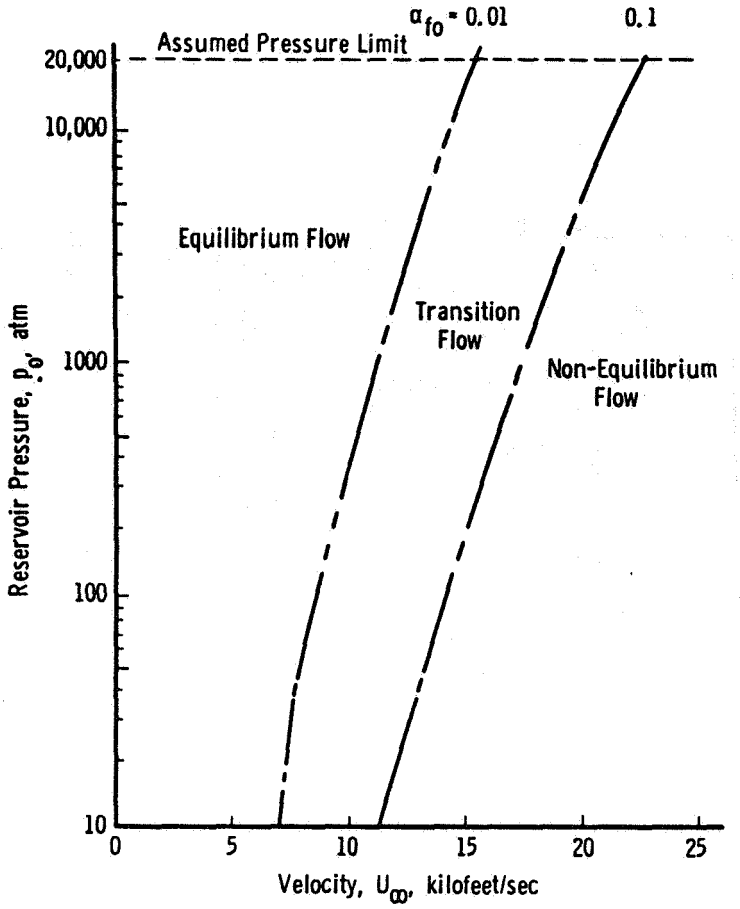

Fig. 5 Reservoir Pressure Required for Equilibrium Nozzle Flow of Air with Oxygen Dissociation

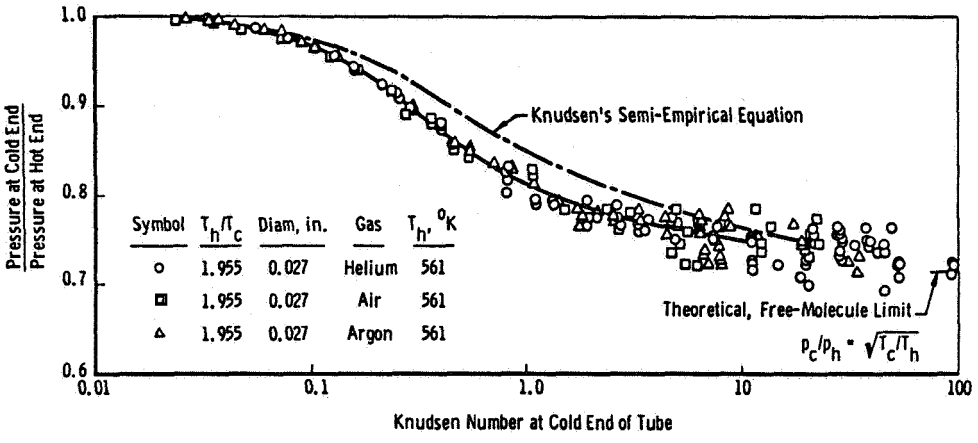

Fig. 6 Thermo-Molecular Flow Effect in Tubes (The symbols p and T represent pressure and temperature, respectively. Subscript c denotes cold end of the tube, and h denotes hot end.)

V-49

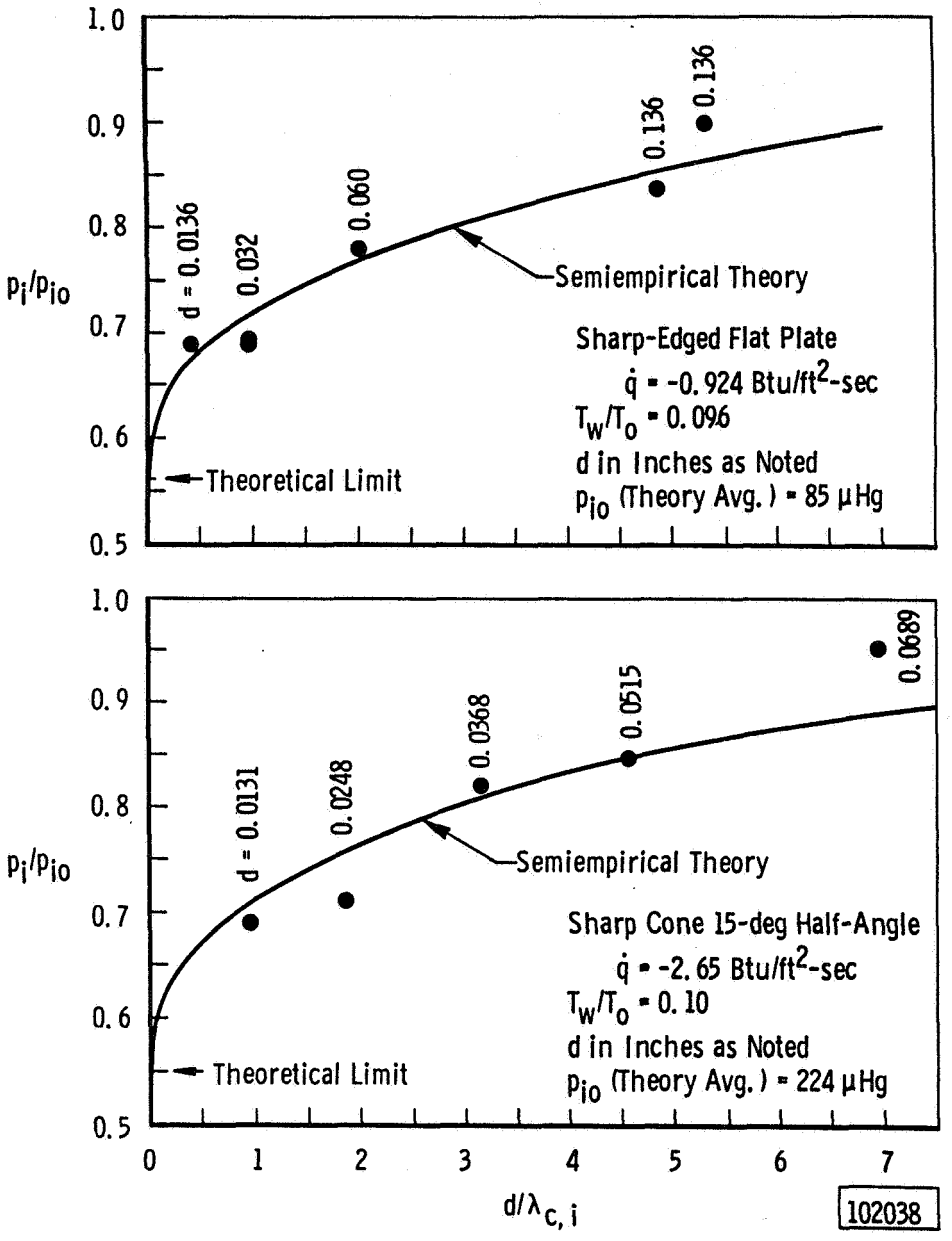

Fig. 7 Measured Static Pressure in Tunnel L (nitrogen gas, M_∞ = 10.15, T_0 = 5620°R, Re_∞ = 388/in., p_i = indicated pressure, p_{io} = true pressure, $\dot{q}$ = heat transfer rate, $\lambda_{c,i}$ = mean free path at p_i and T_c, d = orifice diameter, and T_w = wall temperature.)

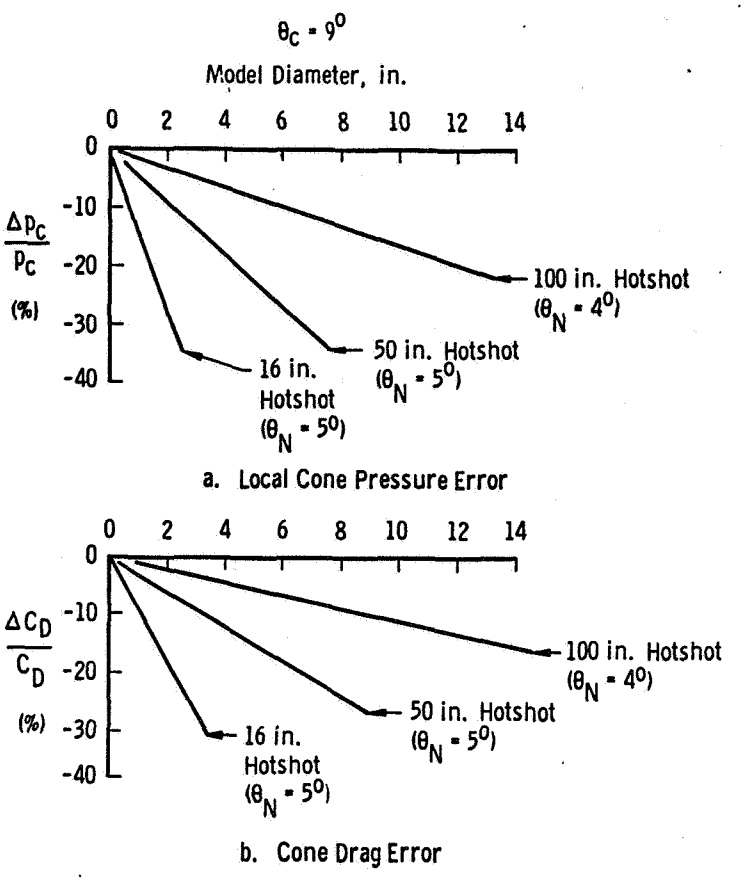

Fig. 8 Theoretical Errors in Cone Pressures and Drag Due to Source Flow over a 9-deg Half-Vertex Angle Cone (p_c = pressure on cone, C_D = drag coefficient, θ_N = nozzle effective expansion angle.)

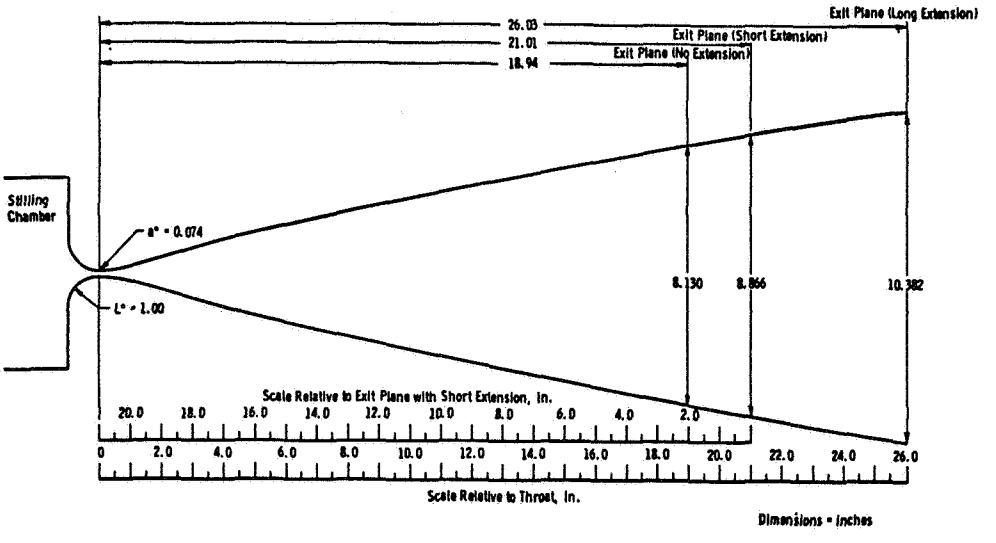

Fig. 9 Tunnel L Nozzle Contour

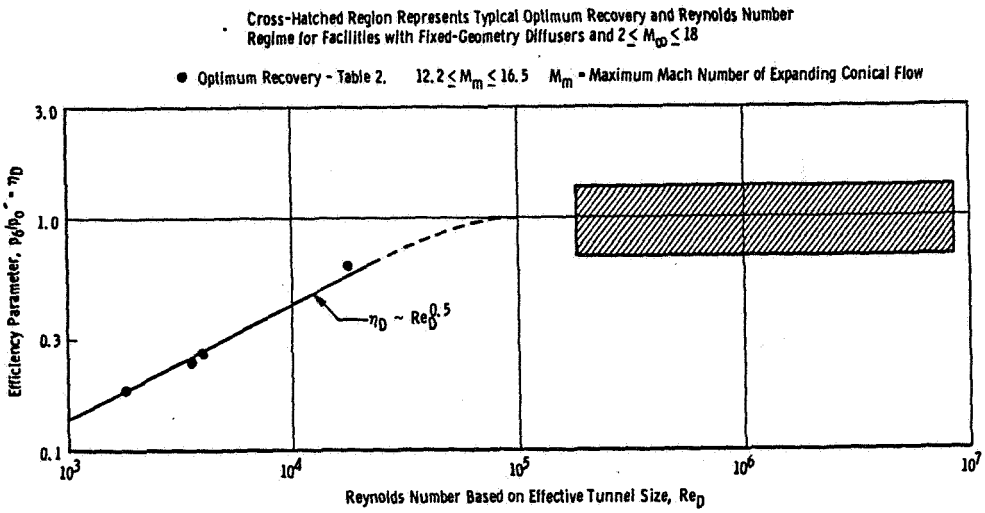

Fig. 10 Diffuser Efficiency as a Function of Reynolds Number (η_D = total pressure ratio across diffuser, Re_D based on stream conditions at M_m and effective diameter of stream expanded to M_m from nozzle throat diameter.)

DATA

○ Tunnel L, August 1962
$\epsilon = 0.175$
$\dot{q}$ = average to entire hemisphere

THEORIES

① Free-molecular flow, diffuse reflection, hypersonic speed, α = accommodation coefficient, normalized to Fay and Riddell.

② Theories of Probstein and Kemp and Van Dyke, normalized to Fay and Riddell for $Re_0 \geq 10^4$ and with Van Dyke's result restricted to $Re_0 \geq 50$. Both theories adjusted to apply to the case $\epsilon = \rho_\infty/\rho_2 = 0.175$.

③ Theory of Cheng, normalized to Cheng's limit for $Re_2 \to \infty$, for $\epsilon = 0.11$. Result of Cheng not strongly affected by ϵ.

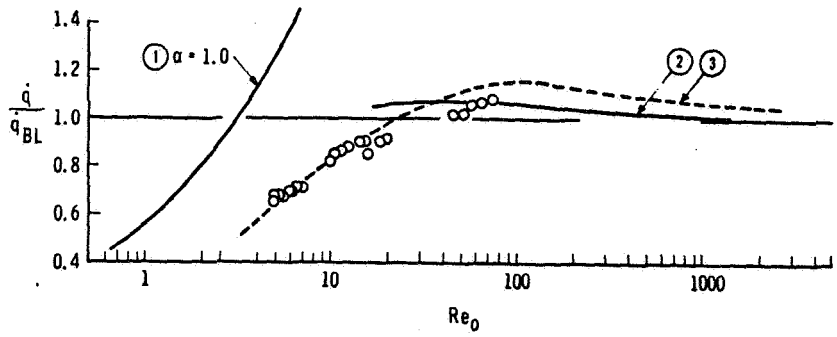

Fig. 11 Heat-Transfer Rates to Hemispherical Noses at Low Reynolds Numbers and Hypersonic Speeds ($\dot{q}$ = Btu/ft^2-sec. $Re_0 = U_\infty \rho_\infty R/\mu_0$ where U_∞ = free-stream velocity, ρ_∞ = free-stream density, R = hemisphere radius, and μ_0 = viscosity corresponding to total enthalpy; ϵ = density ratio across normal shock, subscript BL indicates value calculated by theory of Fay and Riddell.)

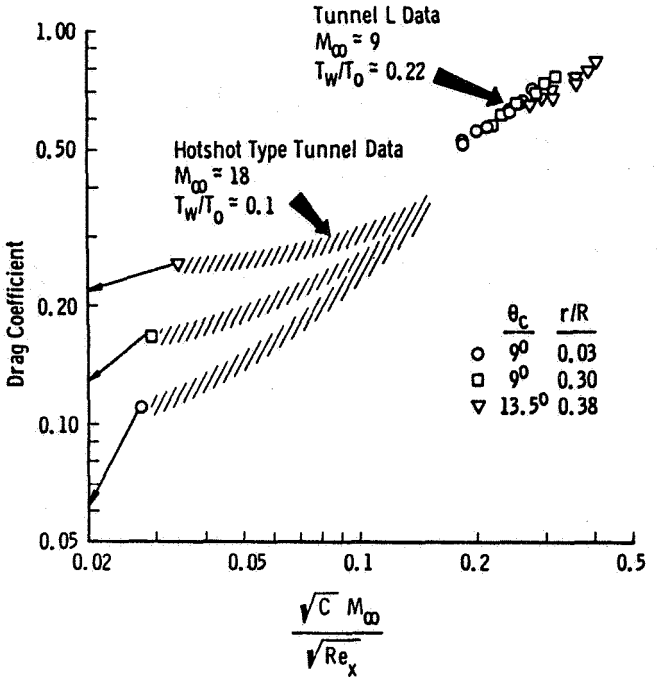

Fig. 12 Drag of Cones at Low Reynolds Number and Hypersonic Speed (Inviscid limits indicated by arrows to ordinate. The ratio of cone nose radius to base radius is denoted as r/R. θ_c = cone half-angle. C = coefficient in linear viscosity-temperature relation, M_∞ = free-stream Mach number, Re_x = Reynolds number based on free-stream conditions and axial length of body.)

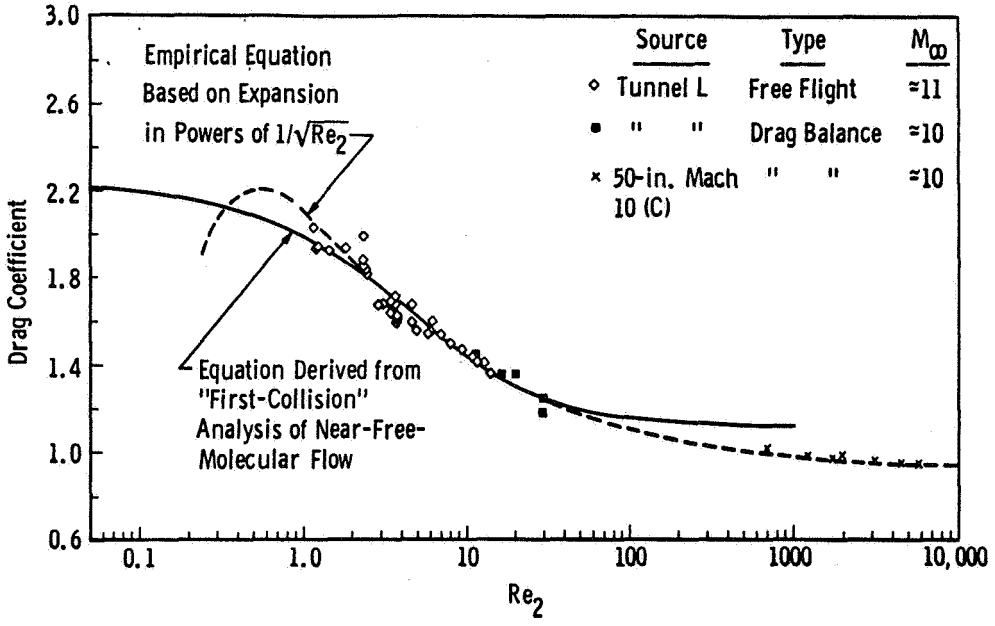

Fig. 13 Drag of Spheres at Low Reynolds Numbers and Hypersonic Speeds (Re_2 is Reynolds number based on conditions immediately downstream of normal shock and sphere diameter, assuming Rankine-Hugoniot shock.)

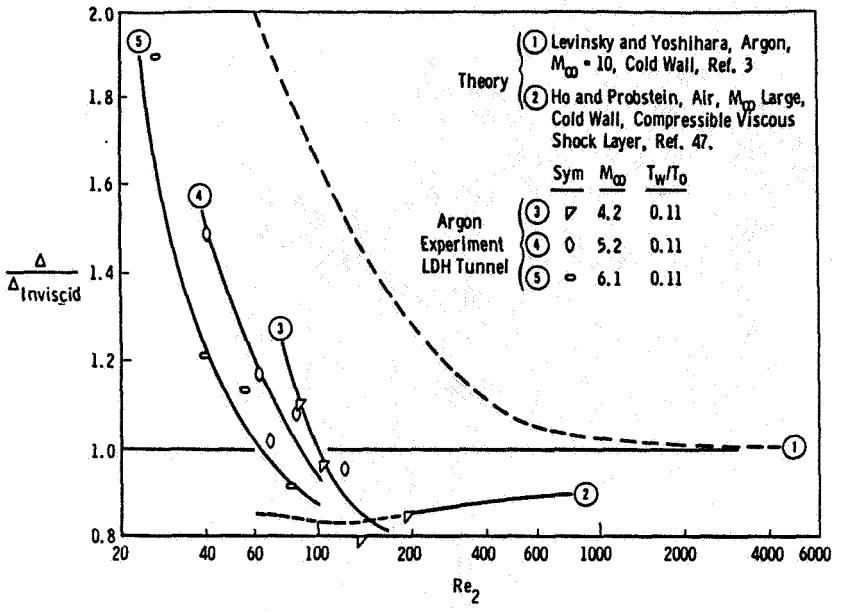

Fig. 14 A Comparison of Theoretical and Experimental Shock Detachment Distances for Hemispheres (Δ is the detachment distance or shock-layer thickness. Re_2 is a Reynolds number based on conditions immediately downstream of a normal shock wave and hemisphere diameter, assuming Rankine-Hugoniot shock.)

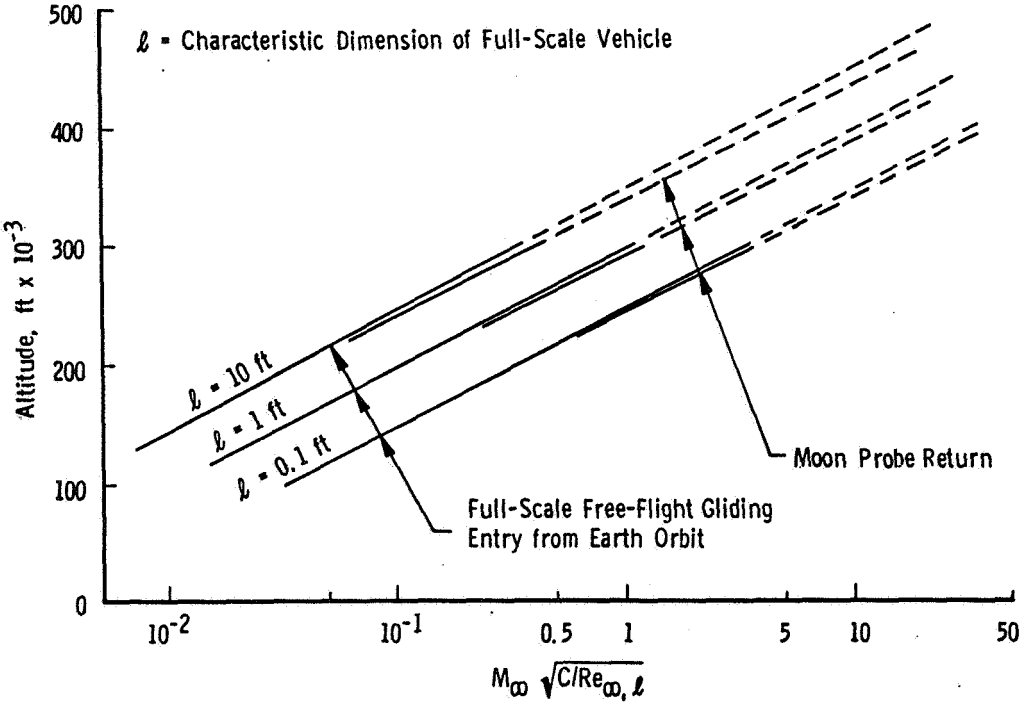

Fig. 15 Viscous Drag Parameter (trajectories of hypothetical, typical, gliding-entry vehicle designs.)

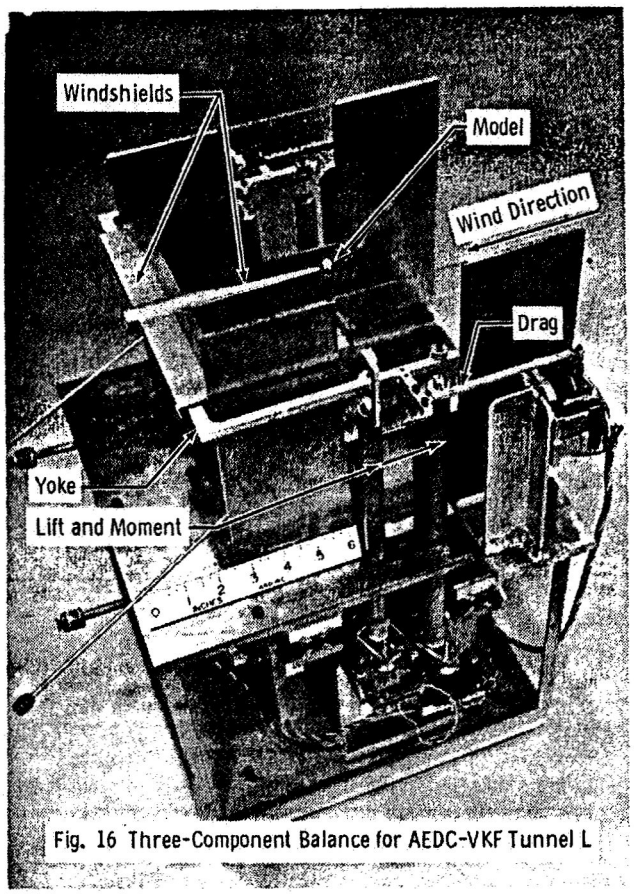

Fig. 16 Three-Component Balance for AEDC-VKF Tunnel L

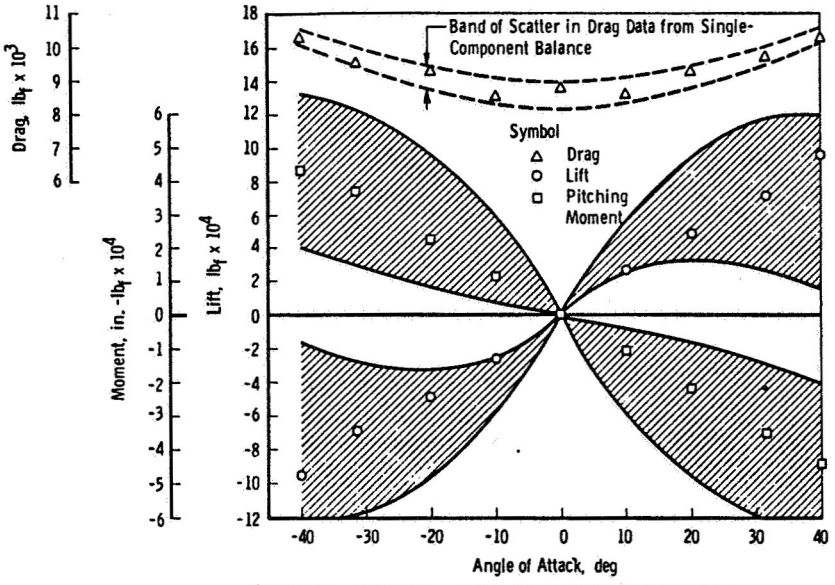

Fig. 17 Example Wind Tunnel Lift, Drag and Pitching Moment Measurements on Blunted Cone (Shaded Regions Lie between Extremes of Free Molecular and Newtonian Theories for Lift and Moment)

Corrected for Orifice Size and Heat Transfer

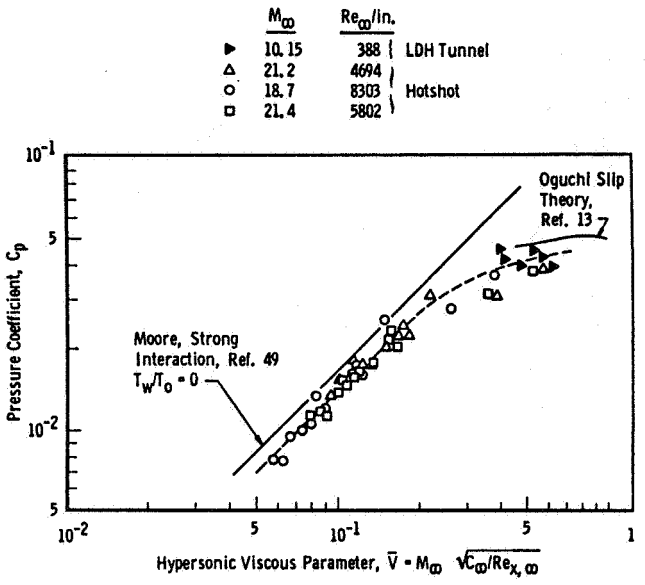

Fig. 18 Hypersonic Viscous Parameter, $\bar{V} = M_\infty \sqrt{C_\infty/Re_{x,\infty}}$ (C_∞ = coefficient in linear viscosity-temperature law, Re_x based on distance to orifice from plate leading edge.)

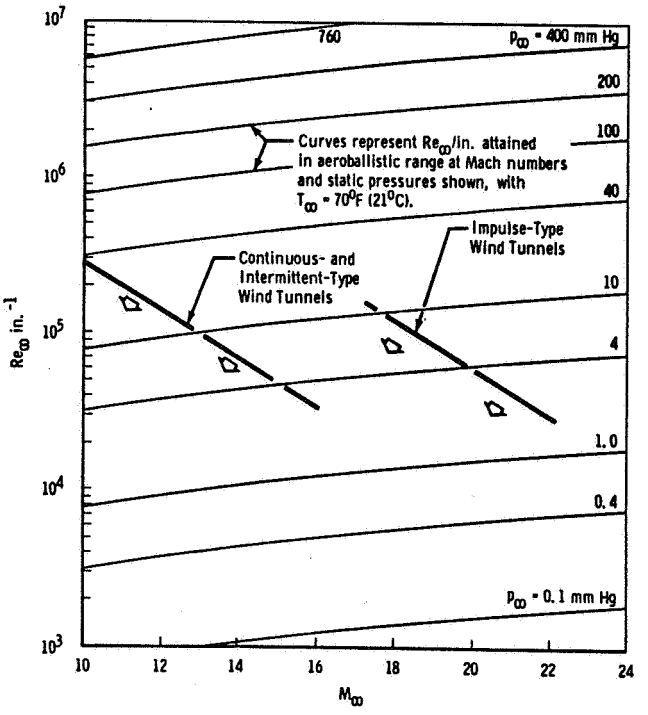

Fig. 19 Unit Reynolds Numbers Currently Available in Hypersonic Wind Tunnels Compared with Aeroballistic Ranges

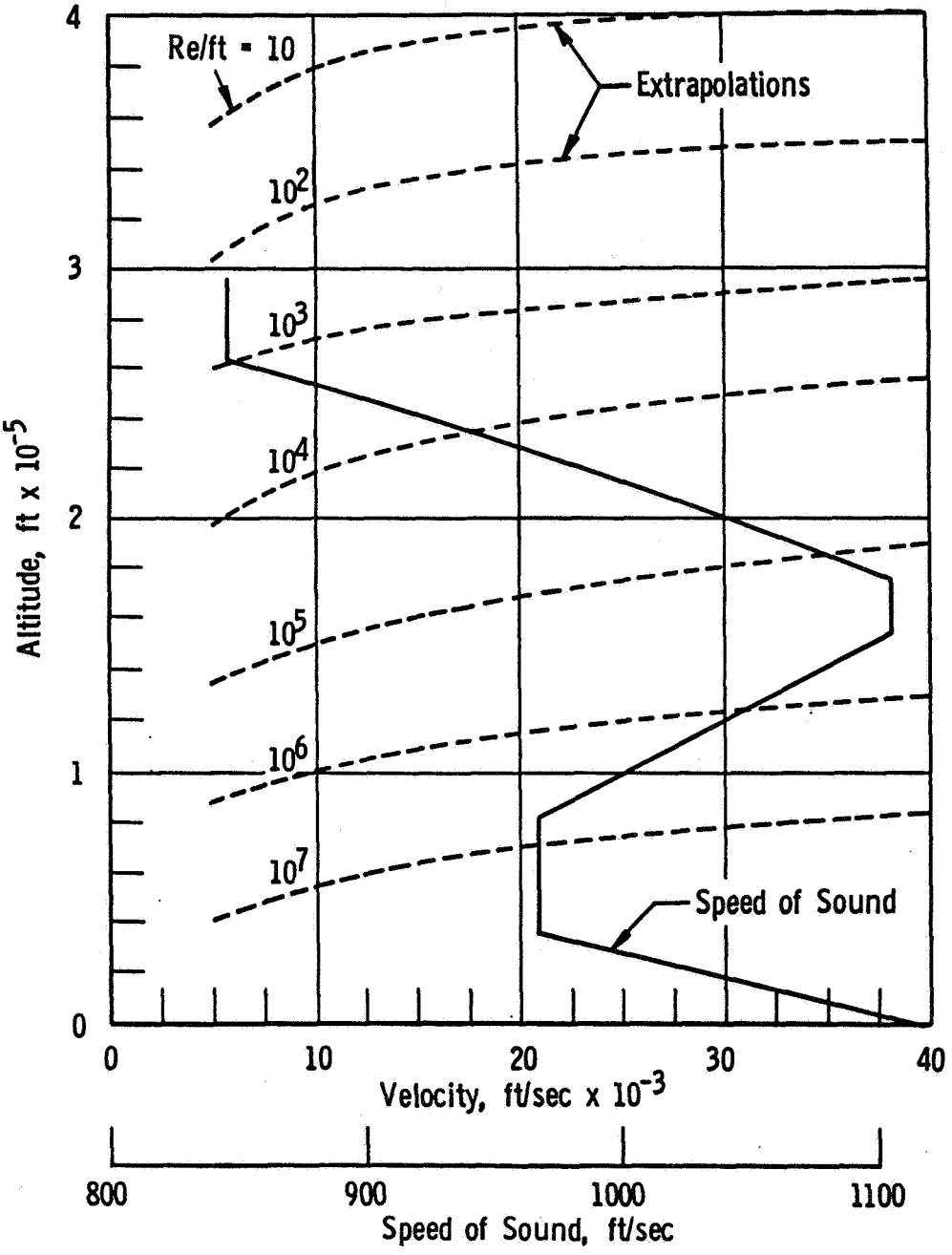

Fig. 20 Selected Data from 1959 ARDC Standard Atmosphere

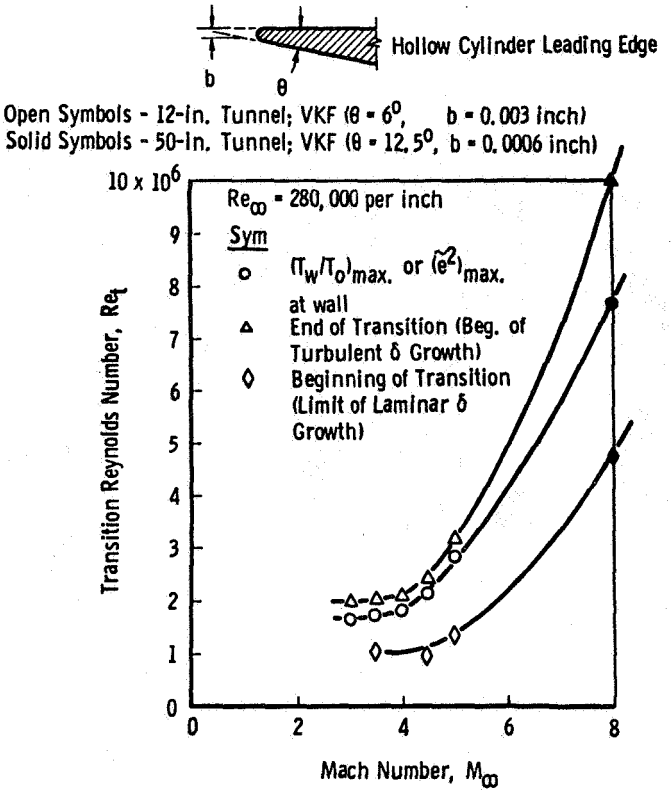

Fig. 21 Influence of Mach Number on Transition Reynolds Number on Exterior of a Hollow Cylinder Aligned with the Flow (T_w = wall temperature, $\tilde{e}^2$ = mean squared fluctuation energy.)

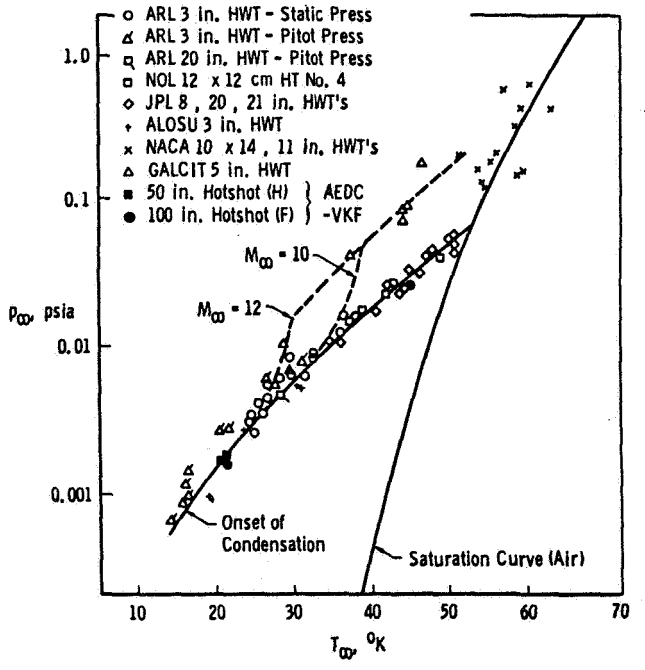

Fig. 22 Phase Diagram

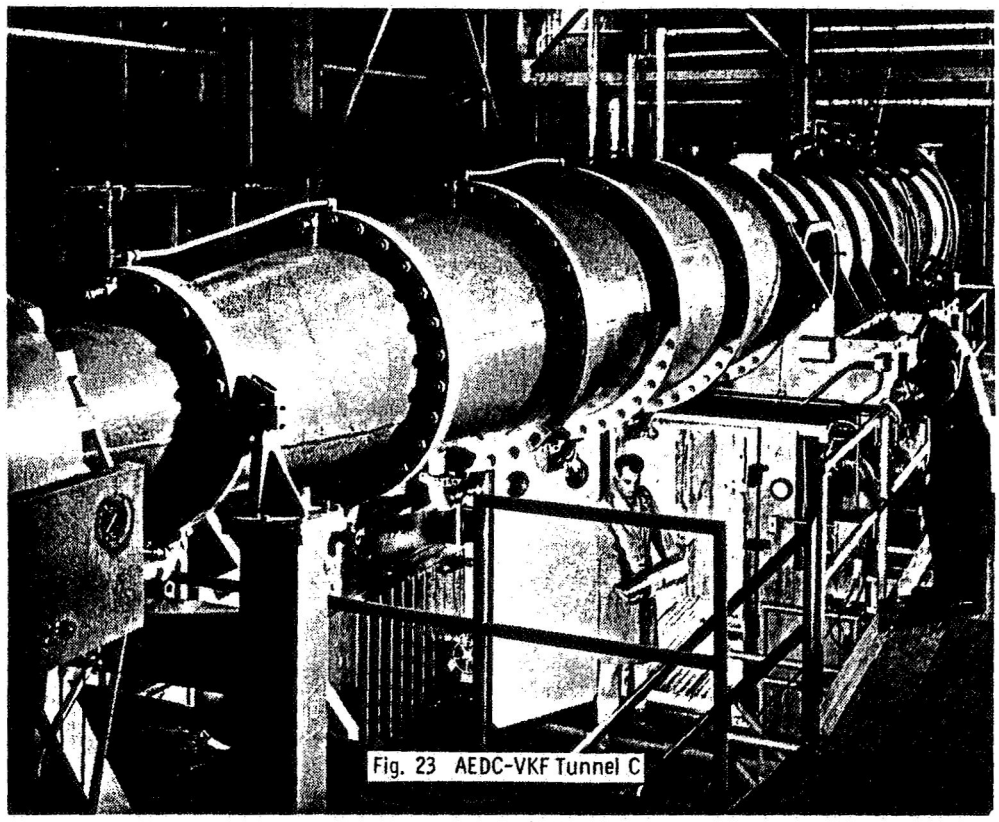

Fig. 23 AEDC-VKF Tunnel C

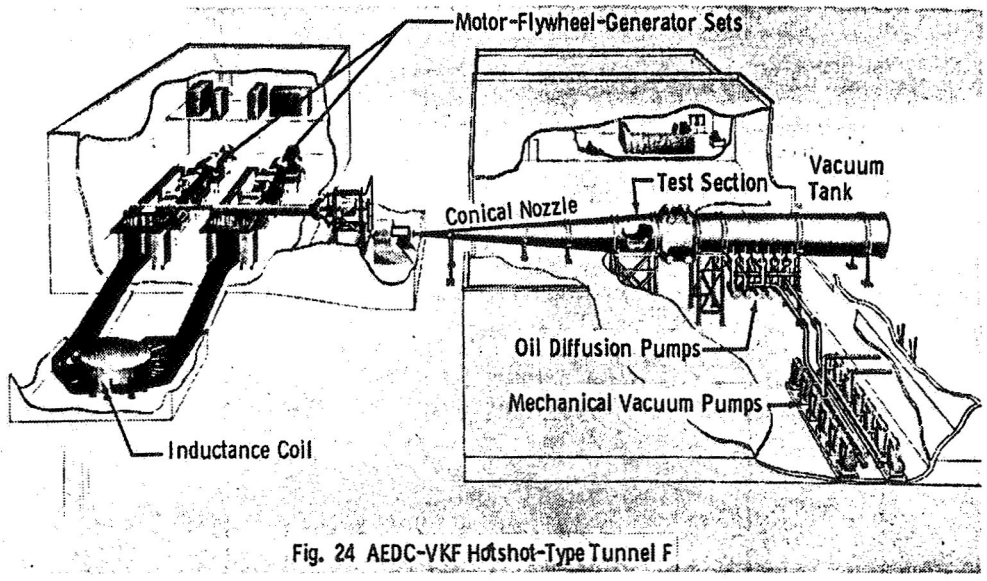

Fig. 24 AEDC-VKF Hotshot-Type Tunnel F

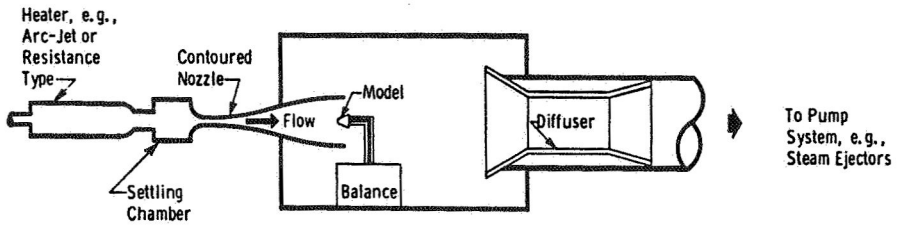

Fig. 25 Schematic of Low-Density, Hypersonic, Continuous-Type Wind Tunnel

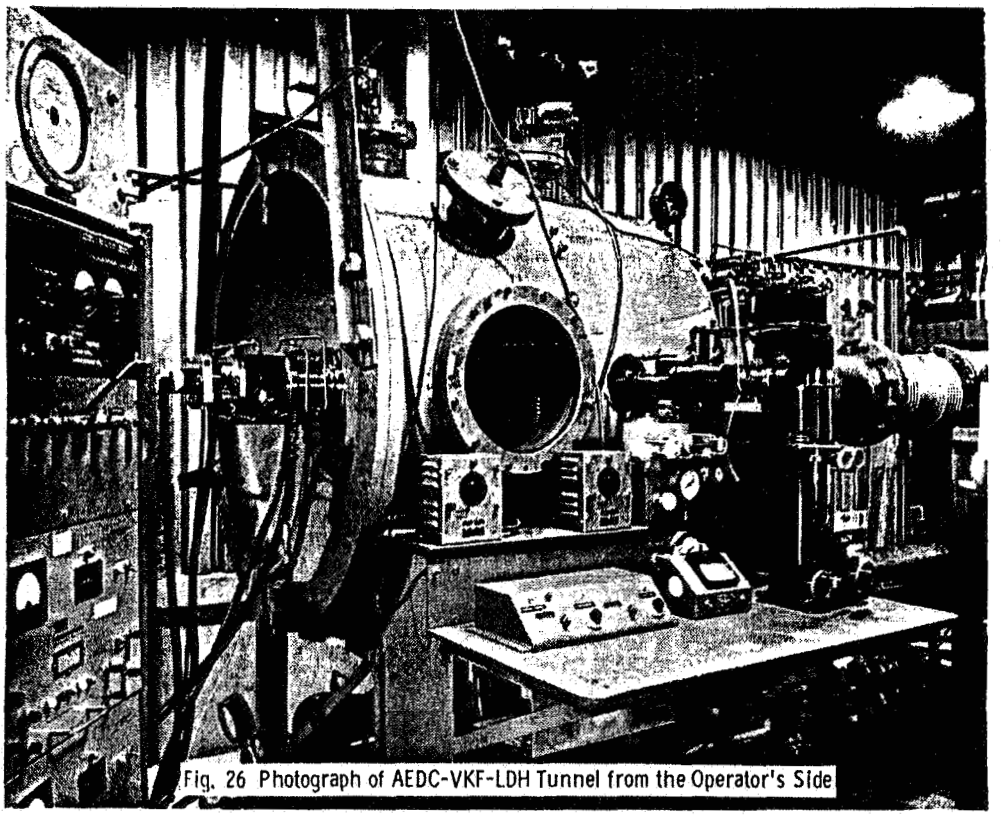

Fig. 26 Photograph of AEDC-VKF-LDH Tunnel from the Operator's Side

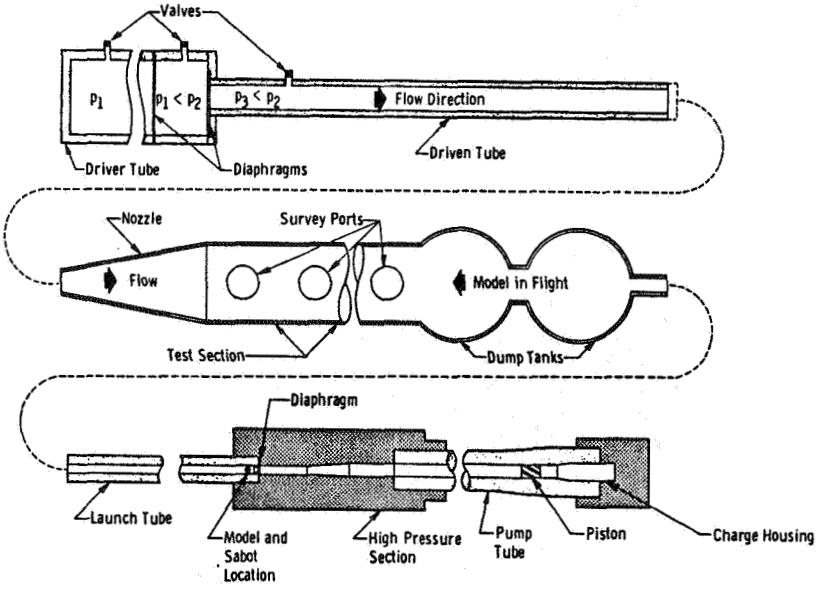

Fig. 27 Schematic of Counterflow Tunnel Components, Also Showing Shock Tube, Shock Tunnel, and Aeroballistic Gun

Vi-60

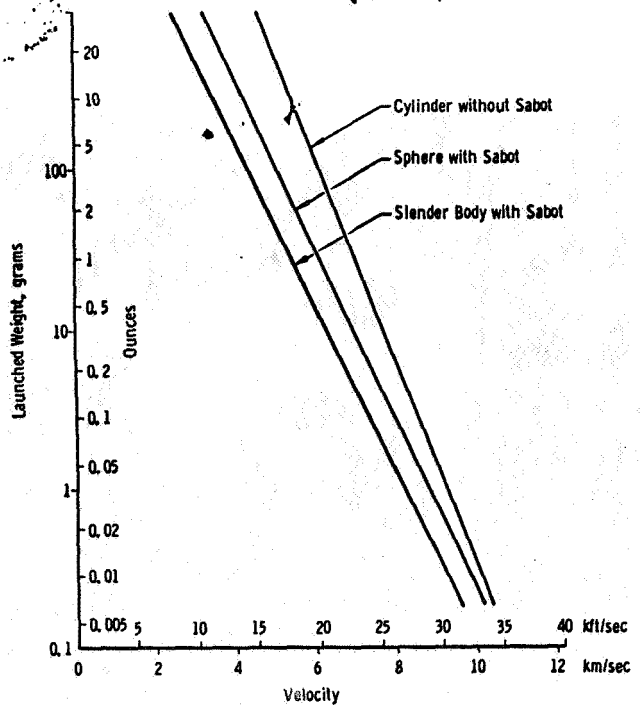

Fig. 28 Current (1964) Status of Aeroballistic Range Launcher Capability

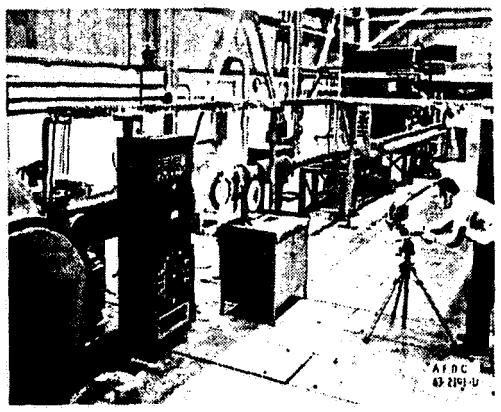

a. Shock Tunnel

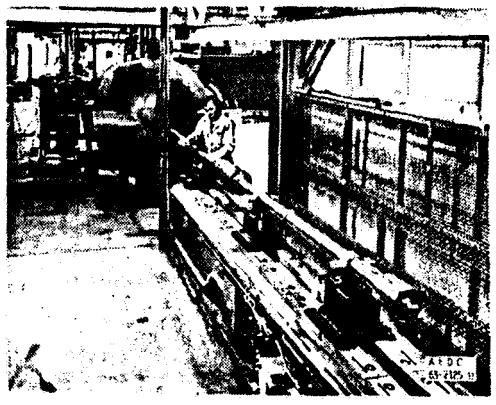

b. Model Launcher

Fig. 29 AEDC-VKF Counterflow Facility